NTNU

Norwegian University of
Science and Technology

Design and operation of a Francis Turbine with Variable Speed Capabilities

Else Høeg Sundfør

Master of Science in Mechanical Engineering
Submission date: June 2017
Supervisor: Pål Tore Selbo Storli, EPT
Co-supervisor: Ole Gunnar Dahlhaug, EPT

Norwegian University of Science and Technology
Department of Energy and Process Engineering

NTNU
Norwegian University
of Science and Technology

Department of Energy
and Process Engineering

EPT-M-2017-85

MASTER THESIS

for

Student Else Høeg Sundfør

Spring 2017

Design and Operation of a Francis Turbine with Variable Speed Capabilities

Design og drift av en Francisturbin med mulighet for variabelt turtall

Background and objective

Recently, it was decided to develop 1000 MW of wind energy in the middle part of Norway. Increasing the admission of intermittent energies like wind and solar into the grid implies that the hydropower turbines necessary for balancing production and consumption must become more flexible. The most non-flexible limitation for current hydropower turbines is the fixed speed due to the use of synchronous generators. If the turbines could be operated with variable speed capabilities, they could be operated as flywheels in case of shut down of intermittent energies, provided much needed power for a short duration until the over-all production can be increased. This could significantly help the green transition by allowing for more intermittent energies to be included into the grid. Furthermore, the over-all efficiency could be improved because the rotational speed could be matched to pressure and flow conditions in a better way.

Objective:
Optimise a design for a runner intended for variable speed operation at a specific hydropower plant, and perform simulations in order to determine the hill chart of this runner. Compare with hill chart for the existing runner as well as obtaining an efficiency gain due to the variable speed operation based on a historical operation.

The following tasks are to be considered:

1. Literature study on turbine characteristics and variable speed operation
2. Use existing software to seek to optimise the hill chart for a new runner design for variable speed operation
3. Compare with a hill chart for an existing runner and use a historical operation as input for determining the energy gain from the variable speed design and operation
4. The previous project work and the future work in this thesis shall be described in a paper which will be presented at 7th International symposium on Current Research in Hydraulic Turbines (CRHT-VII) at Kathmandu University in April 2017.

-- ” --

Within 14 days of receiving the written text on the master thesis, the candidate shall submit a research plan for his project to the department.

When the thesis is evaluated, emphasis is put on processing of the results, and that they are presented in tabular and/or graphic form in a clear manner, and that they are analyzed carefully.

The thesis should be formulated as a research report with summary both in English and Norwegian, conclusion, literature references, table of contents etc. During the preparation of the text, the candidate should make an effort to produce a well-structured and easily readable report. In order to ease the evaluation of the thesis, it is important that the cross-references are correct. In the making of the report, strong emphasis should be placed on both a thorough discussion of the results and an orderly presentation.

The candidate is requested to initiate and keep close contact with his/her academic supervisor(s) throughout the working period. The candidate must follow the rules and regulations of NTNU as well as passive directions given by the Department of Energy and Process Engineering.

Risk assessment of the candidate's work shall be carried out according to the department's procedures. The risk assessment must be documented and included as part of the final report. Events related to the candidate's work adversely affecting the health, safety or security, must be documented and included as part of the final report. If the documentation on risk assessment represents a large number of pages, the full version is to be submitted electronically to the supervisor and an excerpt is included in the report.

Pursuant to "Regulations concerning the supplementary provisions to the technology study program/Master of Science" at NTNU §20, the Department reserves the permission to utilize all the results and data for teaching and research purposes as well as in future publications.

The final report is to be submitted digitally in DAIM. An executive summary of the thesis including title, student's name, supervisor's name, year, department name, and NTNU's logo and name, shall be submitted to the department as a separate pdf file. Based on an agreement with the supervisor, the final report and other material and documents may be given to the supervisor in digital format.

☐ Work to be done in lab (Water power lab, Fluids engineering lab, Thermal engineering lab)
☐ Field work

Department of Energy and Process Engineering, 15. January 2017

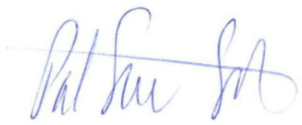

Pål-Tore Storli
Academic Supervisor

Research Advisor: Ole Gunnar Dahlhaug

Preface

This thesis has been written as a requirement for the Master of Science degree in Mechanical Engineering at NTNU during the spring of 2017.

A part of the requirement of writing this thesis was to attend and deliver a paper about the previous project work and the future work in this thesis at the International Symposium on Current Research in Hydraulic Turbines (CRTH) - VII'17. The Symposium is a yearly event organized and held by the turbine testing lab at Kathmandu University, and master students from the hydropower lab at NTNU participates every year. In addition to delivering a paper regarding my project, I was able to present my thesis at the Symposium. Both gave great learning experience, and many people showed interest in the field I have been working on.

The trip to Nepal lasted for a total of three weeks where we visited several different hydropower plants and dam sites as well as technological institutions and primary schools. The trip was partly sponsored by NTNU and private firms engaged in the hydropower sector, and I am very grateful for this educational and enjoyable experience. The paper written for the Symposium and additional information on the symposium can be found in Appendix A.

This thesis presents simulations of a design similar to the Tokke prototype turbine, located in Telemark County. The original design is altered to make it more suitable for variable speed operation. To be able to perform these simulations, a significant amount of my time has been used to learn the computational fluid dynamics program ANSYS CFX. Learning and understanding ANSYS CFX as well as getting reliable results have consumed a lot more time than expected, which have led to significant delays of the simulations. The delays resulted in fewer simulated designs than what was originally desired by the author. Only one new design was simulated.

It is assumed that the reader has a general understanding of fluid mechanics and hydropower technology. I have used the in-house turbine design program Khoj to create and alter the turbine design. Software used to post-process and display the results is ANSYS post, MATLAB and Microsoft Excel. It is noted that it is not necessary for the reader to have knowledge of these programs to understand this report.

Else Høeg Sundfør
Trondheim, June 11th 2017

Acknowledgments

I would like to acknowledge and extend my gratitude to my supervisor Pål-Tore Selbu Storli for creating this exiting task in what I believe is an under studied field. Pål-Tore and my co-supervisor Ole Gunnar Dalhaug have regularly assisted me through both my pre-project and master thesis. A special thank goes out to industrial Ph.D. candidate Erik Os Tengs. He has constantly helped me with ANSYS CFX and given me a lot of insight to the CFD-world. Ph.D. candidate Igor Iliev who are currently writing his doctorate on the same subject has also been a great help along the way with his ideas and knowledge on the subject.

Further, I would like to thank Simen Vogt-Svendsen and Jørgen Ramdal employees in Statkraft for providing power generation data for the turbines at Tokke Power plant as well as efficiency curves. I also have to thank Chirag Trivedi for providing experimental data from the Francis-99 project.

Fellow master student Aase Melaaen have helped me create the MATLAB codes that are used to process the data and create the Hill charts in this thesis. Thank you for sharing your knowledge and patience.

Finally, special thanks go to my fellow students and employees at the hydro lab at NTNU. You have made my last year as a student a memorable and fantastic experience. I will never forget you.

Abstract

Statkraft recently decided to develop 1000 MW of wind energy in the middle of Norway. Wind power is an unreliable energy source. Hydropower is therefore needed to balance energy production supplied to the grid. However, it is limited how much hydropower production can vary because the turbines are designed for a certain operating range. Currently, the most limited variable in hydropower is synchronous speed. It is believed that variable speed operation can yield higher overall efficiencies in a larger operating range.

The objective of this thesis is to optimize a design for a runner intended for variable speed operation for a particular hydropower plant and perform simulations to determine the hill chart for this runner. The possible efficiency gain with variable speed operation is to be determined. This thesis presents simulations of a design similar to the Tokke prototype turbine, located in Telemark County. Then the original design is altered to make it more suitable for variable speed operation.

A design that resembles the Tokke prototype and model have been created and simulated in ANSYS CFX. This design is referred to as design 1 in the thesis. The hill diagram obtained from this design has been compared with the experimental hill diagram of the model turbine in the laboratory. The two hill diagrams do not correlate. However, for n =375 when efficiency is plotted against power output, the shape of the two curves are quite similar. The shape of the curve also correlates well with historical data from the Tokke prototype. For n =375 the average deviation of efficiency between design 1 and experimental model is approximately 2.25%. It seems like neither the model nor the design 1 would have an efficiency gain if the speed could have been adjusted.

From the reviewed literature it comes forth that pump turbines show a higher efficiency increase when operated at variable speed. Pump turbines are designed with higher values of $\underline{u}_1$, than regular Francis turbines. A second simulation design was made, design 2, where $\underline{u}_1$ were changed from 0.72 to 0.80. $\underline{u}_1$ was the only parameter changed from design 1. This change leads to a different runner geometry and inlet dimensions. The comparison between design 1 and 2 show that design 1 has higher efficiencies in the normal operating ranges, as well as high load operational areas. Design 2 gives higher efficiencies in part load operational areas. If the speed could have been adjusted, design 2 shows a maximum efficiency increase of 1.2%.

Due to several simplifications both in the design stage, numerical setup and the choice of steady state solver the numerical results cannot be trusted. Thus, design and numerical setup must be further improved and validated with experimental results. However, the results in this thesis show a promising possible trend for variable speed operation.

Sammendrag

Statkraft har nylig besluttet å utvikle 1000 MW vindkraft i Midt-Norge. Vindkraft er en upålitelig energikilde. Vannkraft er derfor nødvendig for å balansere energiproduksjonen tilført strømnettet. Det er imidlertid begrenset hvor mye vannkraftproduksjon kan variere fordi turbinene er konstruert for et bestemt driftsområde. Den nåværende mest begrensede variabelen i vannkraft synkront turtall. Det antas at drift med variabelt turtall kan kunne gi høyere total virkningsgrad i et større driftsområde.

Målet med denne oppgaven er å optimalisere et design for et turbinblad som er bedre tilpasset variabel turtall operasjon for et bestemt vannkraftverk. Det har blitt utført simuleringer for å bestemme virkningsgraddiagrammet for dette turbinbladet. Den mulige økningen i virkningsgraden med variabel turtall skal bestemmes. Turbinene på Tokke kraftverk ble valgt for rekreasjon og simulering i denne oppgaven.

Et design som ligner Tokke-prototypen og modellen er laget og simulert i ANSYS CFX. Dette designet kalles design 1 i avhandlingen. Virkningsgraddiagrammet laget fra dette designet er sammenlignet med det eksperimentelle virkningsgraddiagrammet til modellturbinen i laboratoriet. De to diagrammene tilsvarer ikke hverandre men, for n = 375 når virkningsgrad er plottet mot effekt, er formen på de to kurvene ganske liknende. Formen på den kurvene korrelerer også godt med historiske data fra Tokke-prototypen. For n = 375 er gjennomsnittlig avvik av virkningsgraden mellom design 1 og den eksperimentelle modellen ca. 2,25%. Det virker som om ikke modellen eller design 1 ville hatt noen økning i virkningsgrad dersom turtallet kunne blitt justert.

Fra omtalt litteratur fremgår det at pumpeturbiner viser en høyere økning i virkningsgrad når de opereres med variabelt turtall. Pumpeturbiner er designet med høyere verdier av $\underline{u}_1$ enn vanlige Francis turbiner. Et nytt simuleringsdesign ble derfor laget som ble kalt design 2. I dette designet ble $\underline{u}_1$ ble endret fra 0,72 til 0,80. $\underline{u}_1$ var den eneste parameteren endret fra design 1. Denne endringen fører til en annerledes geometri på turbinbladene samt endrer innløpsdimensjonene. Sammenligningen mellom design 1 og 2 viser at design 1 har høyere virkingsgard i de normale driftsområdene, samt operasjonsområder med høy belastning. Design 2 gir høyere virkningsgrad i delbelastede operasjonsområder. Hvis hastigheten kunne vært justert, viser design 2 en maksimal økning i virkningsgrad på 1,2%.

På grunn av flere forenklinger både i designtrinnet, numerisk oppsett og valget av en simulering som var simulert i stasjonær tilstand, er ikke de numeriske resultatene til å stole på. Dermed må design og numerisk oppsett forbedres og valideres ytterligere med eksperimentelle resultater. Resultatene i denne oppgaven viser imidlertid en lovende trend for operasjon med variabelt turtall.

Table of Contents

List of Figures

List of Tables

Nomenclature

Symbols

Symbol	Description	Unit
A	Area	[m^2]
B	Height	[m]
c	Absolute velocity	[m/s]
D	Diameter	[m]
f	Frequency	[Hz]
g	Gravity acceleration	[m/s^2]
H	Head	[m]
$\dot{m}$	Mass flow rate	[kg/s]
n	Speed of rotation	[rpm]
p	Pressure	[Pa]
Q	Flow rate	[m^3/s]
t	Thickness	[m]
u	Peripheral velocity	[m/s]
U	Velocity vector $U_{x,y,z}$	[-]
z	Number	[-]
α	Guide vane angle	[°]
β	Blade angle	[°]
ω	Omega	[rad/s]
η	Efficiency	[-]
ρ	Density	[kg/m^3]
τ	Torque	[Nm]

Subscripts

b	Blades
e	Effective
ED	Dimensionless
h	Hydraulic
le	Leading edge
m	Meridional
n	Nominal
p	Poles
$prot$	Prototype
te	Trailing edge
tot	Total
u	Peripheral
1	Inlet
2	Outlet

Abbreviations

CFD	Computational fluid dynamics
BEP	Best efficiency Point
GV	Guide vane
KU	Kathmandu University
NTNU	Norwegian University of Science and Technology
NVE	Norges vassdrags- og energidirektorat
SST	Shear stress transport

1 Introduction

1.1 Hydropower in Norway

Norges vassdrags- og energidirektorat (NVE) has estimated that the Norwegian hydropower potential is approximately 214 TWh/year as of January 2014. Out of that, 132 TWh/year is already built, 49.5 TWh/year includes protected river systems and 0.9 TWH/year is on projects that have been rejected and is therefore not available for development [1]. The remaining hydropower potential, which has not been protected against development, is 33.8 TWh/year. By upgrading existing hydropower plants another substantial part of the hydropower potential can be exploited. Upgrades involve modernizing existing plants into utilizing more of the potential energy in water, this is possible by for example using modern turbine and generator technology.

The average age of large hydropower plants and dams is currently 46 years [1], but this age is increasing, and the old plants will in the near future be in need for upgrades. From an environmental point of view, upgrading is considered the most favorable kind of project, as the environmental impact is small.

1.2 Computational Fluid Dynamics (CFD)

Computational fluid dynamics is a simulation tool used by engineers and physicists to forecast or reconstruct the behavior of a physical situation under assumed or measured boundary conditions. The importance of CFD is many folded and especially important in the design and development phase. In the future, it will be possible to create more realistic simulations as the computer speed, and memory capacity continues to increase over time, Moores Law 1965 [2]. The ability to accurately forecast the performance of a product is becoming more important every day. In addition to this, the only alternative to simulations are experiments which are much more costly or sometimes even impossible to carry out [3]. Simulations can also give much more insight than experiments as it can yield a practically unlimited level of detail in the results [3]. There are many different CFD software packages, both open source and commercial. ANSYS CFX has been chosen for this thesis because it is user friendly and NTNU offers licenses.

All CFD codes contain three main elements: (1) a pre-processor, (2) a solver and (3) a post processor. The functions of these three are briefly explained here.

Pre-processor – Over 50% of the time in the CFD industry is spent in the pre-processing stage [4]. It includes defining the geometry, grid generation and selecting the physical and chemical phenomena that need to be modeled. Also, the fluid properties and the boundary conditions are defined at the domain boundary.

Solver – There are several different numerical solver techniques. ANSYS CFX uses the finite volume method. First, there is an integration of the governing equations of fluid flow over all the control volumes of the domain. Then the discretization takes place followed by the solution of the algebraic equations by an iterative method.

Post-processor – The post-processing stage involves analyzing and visualizing the result with different methods like contour plots, vector plots, streamlines, pressure gradients etc.

1.3 Objective

The objective of this thesis is to optimize a design for a runner intended for variable speed operation for a specific hydropower plant and perform simulations to determine the hill chart for this runner. The specific turbine that is chosen for modification is one of the turbine prototypes at Tokke Power plant, in Telemark County Norway. The reason for choosing the Tokke Power plant was because there is a model of this turbine in the water laboratory at NTNU. The model is scaled down 1:5.1 [5].

A design that resembles the prototype and model will be created and simulated. The hill chart obtained from this design will then be compared with the experimental hill chart of the model turbine in the laboratory. This comparison is conducted to see how well the simulated data matches the experimental data. Then, the design that resembles the prototype will be adjusted and changed to examine if there can be a possible overall efficiency gain at variable speed operation.

In general, turbines are designed for the best efficiency point and will further be refferd to as BEP. If the turbine is always operated at the BEP and the BEP is high, it is not necessary to look at a different design. However, the turbines are not always operated at BEP. This can be due to a reduction in the head or low energy prices, so production is less than usual. Overproduction caused by high energy demand could also be one reason for not operating at BEP. When the turbine is not operated at BEP, there will be a drop in efficiency. The power supplier Statkraft has provided historical data from an arbitrary day of operation of the prototype at Tokke and from these data, it comes forth that the turbines are not always operated at BEP, but in the surrounding areas of BEP as well. The exact efficiency values are confidential and have to be normalized but generated power can be presented. With a basis in the historical data as well as experimental data it might be possible to determine a possible efficiency gain.

1.4 Structure of report

The background for this thesis is presented followed by an explanation of previous work that is relevant to this report. Then a literature survey is conducted that presents important literature that has been used to a great extent. Chapter three gives a general explanation of variable and fixed speed technology, benefits that could come from variable speed operation and which design features that might be more suitable for variable speed operations. Chapter four goes into detail about the driving pattern at Tokke power plant. An explanation of how the hill diagrams are created follows in chapter five. In chapter six the numerical modeling is presented including a brief explanation of the turbine design software Khoj, ANSYS meshing software TurboGrid and the simulation solver CFX. Initial design parameters for the Tokke prototype, mesh quality, turbulence model, numerical setup and solver control are among the things discussed in this chapter. Experimental and numerical results and discussion of the results come forth in chapter

seven followed up by a conclusion in chapter eight. At last in chapter nine discussion of the remaining and possible further work is performed.

2 Background

2.1 Renewable Energy

It was recently decided by Statkraft to develop 1000 MW of wind energy in the middle part of Norway. Hydropower is therefore needed to balance intermittent energies like wind and solar on the grid. This means that hydropower have to become more flexible and the main requirement for modern turbines is high efficiency over the whole operating range. The most non-flexible limitation for current turbines is fixed speed due to the use of synchronous generators to provide energy to the fixed-frequency electric grid. If the turbines could be operated with variable speed capabilities, they could be operated as flywheels in the case of shutdown of intermittent energies and provide the needed power for a short duration until the intermittent energy sources start producing again. Overall efficiency could also be improved because the rotational speed could be matched to pressure and flow conditions in at better way.

2.2 Previous work

Francis-99 is a series of three workshops where two have already been conducted, one in 2014 and one in 2016 and the third workshop is set to be conducted at the end of 2018. The workshops give open access to the complete design and data of a model Francis turbine so that researchers can perform numerical studies on the model. The model is a scaled model of the prototype turbines operating at Tokke power plant. Due to the complex flow structure in the turbine numerical modeling are facing significant challenges. One technique applied to one operating load does not necessarily work for the same turbine at a different operating load. This can make numerical modeling of hydraulic turbines expensive in regards of computational time and power, and the need to optimize CFD modeling to be less costly is of importance.

The focus of the first workshop concentrated around steady state operating conditions where over 50 researchers participated, and 14 papers were presented. During the first workshop, an experimental study was performed on the Tokke model in the laboratory using an open loop hydraulic system. After calibration, the total uncertainty in hydraulic efficiency was ±0.16%. A total of 10 different guide vane angles and 15 different speed values for each angle were selected, which gave the efficiency measurements a total of 150 points. More details of the experimental setup can be found at NVKSs home pages under Francis-99-Experimental study and in “Experimental and Numerical Studies of a High-head Francis Turbine: A review of the Francis-99 test case” by Trivedi, Cervantes and Dalhaug [6]. Most papers involved numerical simulations which were compared with the experimental data provided by the workshop organization. Several of the papers focuses on using different software and turbulence models to recreate the experimental model in as close approximation as possible. In addition to other scientific research. Great help has come from these reports concerning numerical setup, turbulence models, and acceptable simulation solver criteria.

Kristine Gjøsæter made the in-house MATLAB software named Khoj during her master thesis in the spring of 2011. Khoj is the applied design software in this thesis. It was originally made to carry out a hydraulic design of a new Francis turbine with reduced velocities to reduce corrosion in the turbine. Khoj is a Francis design software programmed in MATLAB with a graphical user interface and the background information for the design software can be found in her master thesis – Hydraulic design of Francis Turbine Exposed to Sediment erosion [7].

In the autumn of 2011, Peter Joachim Gogstad in co-cooperation with Kristine Gjøsæter further developed the program by adding some features to it. This includes visual changes, a new option to choose leading edge geometry, blade leaning has been included, and the blade thickness tab has been further developed. Details of the changes can be reviewed in Gogstad's master thesis – Hydraulic design of Francis turbine exposed to sediment erosion [8]. Khoj is presented in further detail in Chapter 5.1.

During the autumn of 2016 industrial Ph.D. candidate, Erik Os Tengs created a link between Khoj and ANSYS CFX. The link makes it possible to do design changes, numerical setup and solving in ANSYS Workbench. One simply choose the design input values, MATLAB calculates and creates the runner geometry and imports it into TurboGrid meshing. This configuration makes the process of adjusting the design very fast and easy. The setup constructed by Tengs have been used in this thesis.

2.3 Literature survey

This chapter presents the main literature that have been used for understanding the basics with the three subjects: Design and simulation software, hydropower turbines and variable speed technology.

2.3.1 Design and simulation software

Gjøsæther's thesis, as well as Gogstad's project work, have been used to understand how the turbine design software Khoj works [7,8].

In this thesis, all simulations are accomplished with three-dimensional Navier-Stokes solver ANSYS CFX 17.2. For general information on CFD the book "An introduction to computational fluid dynamics, the finite volume method", second edition is used to get an introduction to the subject. In addition to this ANSYS has several user manuals that have frequently been used to learn about mesh creation, turbulence models, numerical setup and solver software.

SHARCNET is the largest high-performance-computing consortium in Canada, including 18 universities, colleges and research institutes across southwest, central and northern Ontario. This website contains a lot of information on ANSYS CFX concerning meshing and mesh quality, which also has frequently used during the thesis along with ANSYS user manuals.

2.3.2 Hydropower turbines

For general information on turbine and pump design "Pumper og Turbiner" from 2003 and "Grunnkurs i hydrauliske strømningsmaskiner" from 2000, both written by, Hermod Brekke have

been used to great extent to get an insight into the turbine design process. The design process described in Brekke is very similar to the design procedure utilized in Khoj. Lecture notes from the subject TEP4195-Turbomachinery and Mechanical equipment by Arne Kjølle have been used to get a general understanding of Francis turbines, power plant equipment and operation.

2.3.3 Variable speed technology

There are few open sources to literature about variable speed technology connected to hydropower turbines. In general, most articles only explain what could be the benefits of variable speed operation, but does not give any indication about the design features of the turbines. Only one article by Farell and Gulliver [9] from 1987 was found regarding design aspects and what type of turbines that might benefit from variable speed operation.

3 Variable speed technology

3.1 Fixed speed topology

In a conventionally fixed speed turbine, the magnetic field of the stator and the magnetic field of the rotor are coupled and always rotates with the same speed. As the grid frequency is constant, the speed of the generator, hence also the speed of the turbine is given by Equation 3.1.

$$n = \frac{120 \cdot f_{grid}}{z_p} \tag{3.1}$$

Where n is the rotational speed, f_{grid} is the frequency of the grid and z_p is the number of poles in the generator. A turbine that uses fixed speed technology is designed for an optimum value of head and discharge, and any variation of these parameters will drive the turbine to an efficiency value lower than the optimum value.

3.2 Variable speed topology

In locations where it is economical and desired to run the turbine at optimum efficiencies, but there are large variations in head or discharge, variable speed operations is required. In a variable speed machine, the stator and the magnetic field of the rotor are decoupled. Either the stator is decoupled from the grid using a frequency converter between the grid and the stator winding, or the rotor field is decoupled by a multiphase rotor winding fed from a frequency converter connected to the rotor [10].

3.3 Benefits with variable speed operation

The hydraulic efficiency depends significantly on both the water discharge, Q and the nominal head, H_n, and is normally represented in a hill diagram illustrated in Figure 1. If n or Q deviates from their nominal values at BEP, the efficiency will drop. This can happen either if the head or flow changes. In addition to a drop in efficiency, some operational problems can arise. Part load fixed speed operation with low heads can result in draft tube oscillations and shaft torque fluctuations. On the other hand high load fixed speed operation can give rise to the appearance of cavitation [11].

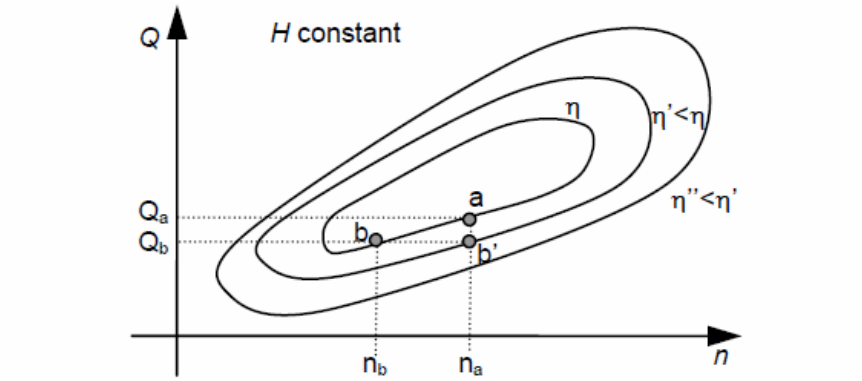

Figure 1 – Example 1 of hill diagram[3]

The idea of variable speed is that if the head or discharge changes, the rotational speed can be adjusted accordingly to maintain high efficiencies. This is demonstrated in Figure 1. For fixed speed operation at a certain head, the efficiency of the turbine will decrease from *a* to *b'* when the discharge decreases from Q_a to Q_b. With variable speed operation, the speed can be adjusted from n_a to n_b to obtain an efficiency in point *b* which is equivalent to the efficiency in point *a*.

Consequently, a variable speed turbine permits maximum efficiency tracking for a given power demand [12]. This kind of operation is only possible if the hill chart looks similar to the one in Figure 1. If the hill chart curve is more symmetrical like in Figure 2, adjusting the speed in either direction will not affect the efficiency. Therefore the goal is an attempt to make a turbine design, which ultimately can yield a hill chart curve that looks similar to the one in Figure 1. However, the design should not be adjusted to such an extent that the hydraulic efficiency becomes significantly lower. The idea is to produce a "stretched" hill chart without significantly lowering the overall efficiencies.

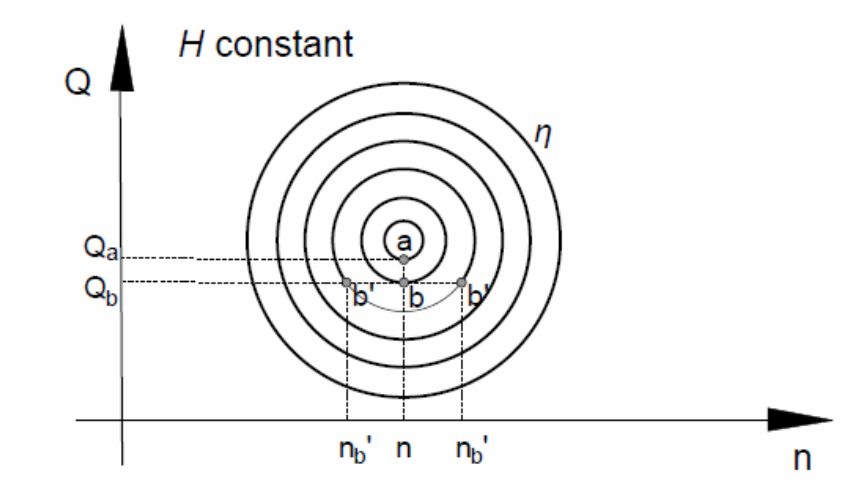

Figure 2 – Example 2 of hill diagram

3.4 Parameters believed to create a "stretched" hill diagram

Farell and Gulliver [9] compared data from 8 different turbines for variable speed performance at constant head. This included two small axial flow turbines with fixed vanes, A_1 and A_2, an axial pump used as a Turbine, P_1, three Francis turbines, F_1, F_2 and F_3, a pump turbine, T_1, and a Kaplan turbine, K_1. The data was obtained from different suppliers or available literature, and the processing of the data was different for each turbine since the original data varied for each turbine.

The three Francis turbines and the Kaplan turbine were given slightly more attention since it is desired to use adjustable guide vanes along with variable speed. However, the results indicated that variable speed would not significantly improve performance at off-design flow and constant head.

The Bureau of Reclamation pump turbine, T_1, was tested with variable gate procedure and revealed significant improvement, which can be viewed in Figure 3. The specific speed of this unit is similar to turbine F_2, which had very limited efficiency improvement.

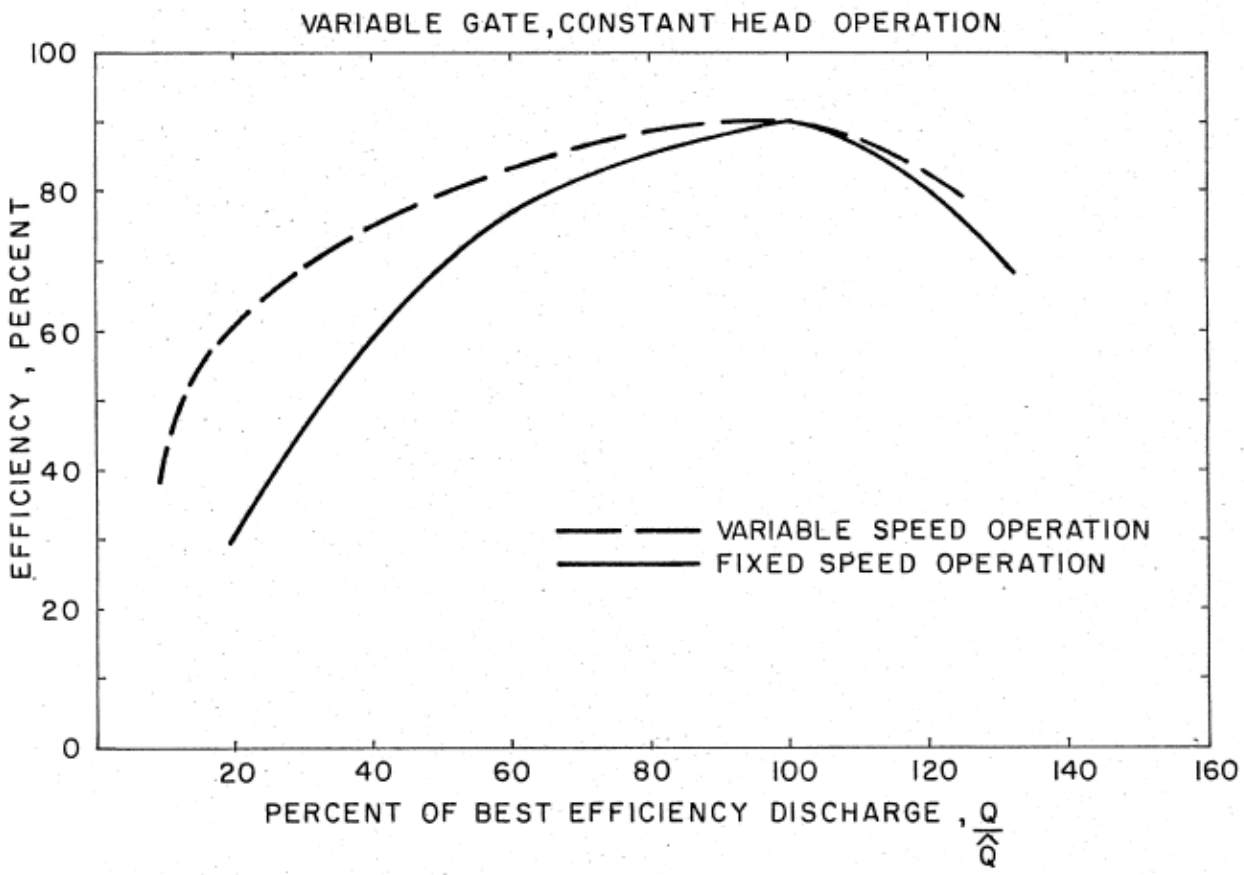

Figure 3 – Variable and fixed-speed characteristics of USBR pump turbine T_1 (N_S=0.76) [4]

The authors cannot pinpoint the reason for the difference when the speed numbers are so similar, but they argue that the different runner geometries and turbine characteristics can affect the variable speed performance. The runner geometry of the pump turbine is closer to the design of a pump than a turbine. For a pump-turbine the runner will be a compromise with lower efficiency than a Francis turbine at BEP and the inlet diagram will resemble an inlet diagram of a pump with a large value of $\underline{u}_1 > 0.95$[13]. For a standard Francis turbine, the value would have been $\underline{u}_1 = 0.72$. A parameter study on $\underline{u}_1$ is therefore conducted in this thesis to see how this parameter will affect the hill diagram curves.

Farell and Gulliver also claim that the turbines with the higher specific speeds had the greatest improvement in performance and exhibited the largest increases in discharge with increasing rotational speed. This statement is not further investigated in this thesis.

4 Creation of Hill Diagram

Hill diagrams for hydropower turbines are created so that something can be said about how the turbine operates in the different operating points. The hill diagrams are created with dimensionless parameters so it can be compared to other rotating machinery, models and prototypes [14]. The dimensionless volume flow Q_{ED} is plotted against the dimensionless rotational speed n_{ED} defined respectively in Equation 5.1 and 5.2.

$$Q_{ED} = \frac{Q}{D_2^2 \cdot \sqrt{gH_e}} \tag{5.1}$$

$$n_{ED} = \frac{(n/60) \cdot D_2}{\sqrt{gH_e}} \tag{5.2}$$

Where Q is the volume flow rate through the entire turbine, D_2 is the outlet diameter, n is the rotational speed, and H_e is the effective head.

To create a hill diagram in the laboratory one keeps the guide vane opening constant while varying the speed. The flow, head and torque are measured, and the efficiency is calculated as the ratio between delivered energy to the turbine shaft and supplied energy. This procedure is repeated for some different guide vane openings. As a rule of thumb, the speed of rotation is regulated in the range of ±20 % from BEP and guide vane opening, α, is regulated in the range of ±40% from BEP when doing measurements [15,16].

Essentially the same procedure is used when creating a hill diagram in ANSYS and MATLAB. A new workbench called Hill was created in ANSYS including a CFX simulation where the design and mesh are imported. The CFX solution setup was then connected to a block called response surface. In response surface, it is possible to run the turbine at different RPM and alpha values. RPM and alpha are selected as input parameters and efficiency, head and mass flow are chosen as output parameters. Alpha is selected to be between 7-13 with a one-degree interval and RPM to be in the range between 355-425 with an interval of 10. It was originally chosen to use the full range as proposed but it was not done due to time limitations.

ANSYS provides the mass flow rate [kg/s] over one runner blade. The mass flow rate has to be converted to volume flow for the whole turbine. Volume flow over the entire turbine is calculated with Equation 5.3.

$$Q = \frac{\dot{m} \cdot z_b}{\rho} \tag{5.3}$$

Where $\dot{m}$ is the mass flow rate through the turbine is, z_b is the number of runner blades and ρ is the density of water.

The MATLAB script that creates the hill diagram is made with help from Aase Melaaen. Essentially Q_{ED} is plotted against n_{ED}, efficiency curves are created, guide vane openings are created as

straight lines and BEP is marked with a red circle. In addition to making the Hill diagram the efficiency is plotted against n_{ED}. The full MATLAB code is attached in Appendix B.

5 Driving pattern at Tokke power plant

Tokke Power plant is located in Telemark County in Norway. Four identical turbines are installed with a total capacity of 430 MW. Simen Vogt-Svendsen (simen.vogt-svendsen@statkraft.com) from Statkraft provided data from Tokke power plant for all four generators for a 24-hour period. The dataset from generator 4 was not complete and had a missing gap of 6 hours. It was therefore chosen to not use the data from this generator. The driving pattern for the remaining three generators were so similar that is was chosen to only further process data from generator 1 and using these data for comparison in the thesis.

Data from the first hour is not included as these power output values are not normal for the turbines. The logging interval is based on change in power output and not time. A more correct way of presenting the driving pattern was therefore made by averaging the power output for each hour and then plotting the power output over each hour.

These data, displayed in Figure 4, illustrates the power output from Tokke on an average hourly basis.

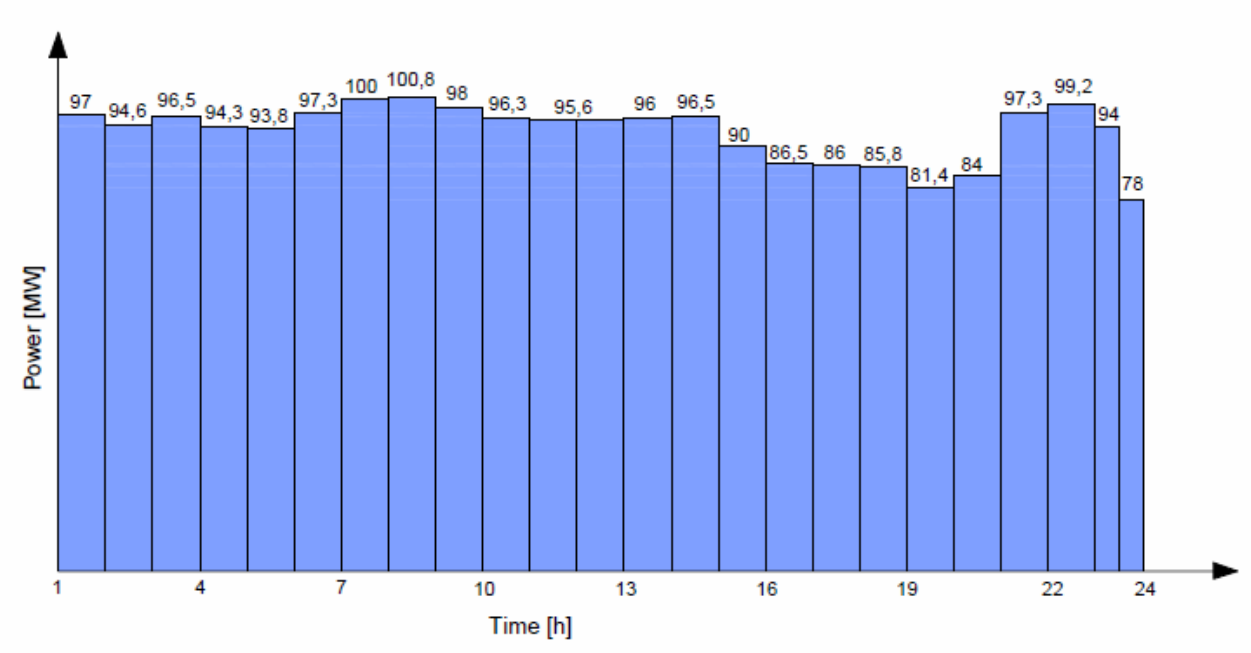

Figure 4 – Averaged power output for each hour for generator 1 at Tokke power plant

On average the turbines produce 83.94 MW 5.5 hours per day, 94.87 MW for 10.5 hours every day and 98.5 MW for 7.5 hours each day. The average power output operating range at Tokke seems from these data to be between 85-100 MW.

6 Numerical modelling

6.1 Turbine design software: Khoj

In 2011, during her master thesis, Kristine Gjøsæter started developing the in-house turbine design software Khoj, which has been further, modified until this day [7, 8]. Khoj is a Francis design software programmed in MATLAB with a graphical user interface. The software is created with the intention of constructing a brand new turbine and follows a specific design procedure; this is relevant to this task and will be explained further in this chapter.

In Khoj one can design the runner, guide vanes, stay vanes and spiral casing. However, in this thesis, it is desired to keep the simulations simple, since this is the design stage phase, and only simulate the flow over the runner blades. Hence only the runner blades are created. A shortened version of the design procedure of the runner blades, as well as explanations for the initial design parameters, will follow below. Background information for the design software and the full design procedure can be found in Gjøsæter's thesis– Hydraulic Design of Francis Turbine Exposed to Sediment Erosion [7].

The main dimensions of the design are based on the hydraulic parameters effective head, H_e, and volume flow, Q. The nominal head is chosen to be 377 m, and the volume flow is set to be 31 m^3/s. H_E will be calculated by ANSYS with basis in the nominal head. These values selected since they are approximately the same as for the prototype at Tokke [17].

In this design processes, one starts with determining the main outlet parameters. It is desired to make the runner design and dimensions similar to the prototype at Tokke. The outlet diameter, D_2, at Tokke is 1.8 m, and it is possible to calculate what c_{m2}, u_2, and β_2 based on the following equations.

$$D_2 = \sqrt{\frac{4Q}{\pi \cdot c_{m2}}} \tag{6.1}$$

From Equation 6.1 the obtained value of c_{m2} is 12.18 m/s. Since there is assumed no swirl at the outlet at BEP the connection between c_{m2}, u_2 and β_2 can be written as in Equation 6.2.

$$c_{m2} = u_2 \cdot tan\beta_2 \tag{6.2}$$

There are some combinations of u_2 and β_2 that would yield the correct value for c_{m2}. Brekke [13] suggests that the values of u_2 and β_2 should be within a certain range. Based on this range u_2 is set to be 38 m/s and β_2 is chosen to be 19°. A small iteration loop is conducted to account for the blade thickness at the outlet correcting the values of u_2 and β_2. Knowing D_2, and having decided a value for u_2 the rotational speed can be calculated by Equation 6.3.

$$n = \frac{u_2 \cdot 60}{\pi \cdot D_2} \tag{6.3}$$

Equation 6.3 gives an initial rotational speed of 403.2 RPM. However, Khoj corrects the rotational speed to get synchronous speed. In this case, it is rounded down to 375 RPM. Synchronous speed is not a requirement for this thesis, but to keep the work load on a realistic level and as it was not part of the objective this is accepted.

Further, the inlet dimensions are calculated. The designer chooses the inlet reduced peripheral velocity, $\underline{u}_1$. Based on the inlet reduced peripheral velocity and the rotational speed, D_1 can be calculated with Equation 6.5.

$$u_1 = \underline{u}_1\sqrt{2gH_e} \tag{6.4}$$

$$D_1 = \frac{u_1 \cdot 60}{n \cdot \pi} \tag{6.5}$$

For this thesis, it is desired to keep D_1 constant to keep the dimensions equal or similar to the prototype at Tokke. However, the way Khoj is coded this will not be possible and D_1 will change. If it at some later point is wanted to rewrite Khoj, it might be possible to keep D_1 constant. Then u_1 could be changed on behalf of changing the rotational speed, n, instead of the inlet diameter, D_1.

For Francis turbines it is common to choose a value of $\underline{u}_1$ between 0.71-0.73 [13]. For the initial design, a value of 0.72 is selected. At BEP there is assumed zero rotation on the outlet and hydraulic efficiency is chosen to be 0.96. C_{u1} can be found by Equation 6.6.

$$\eta_h = 2 \cdot \underline{c}_{u1} \cdot \underline{u}_1 \tag{6.6}$$

To avoid backflow in the runner, acceleration through the runner is desirable. An acceleration of 10 percent is chosen, and c_{m1} is calculated by Equation 6.7.

$$c_{m1} = \frac{c_{m2}}{1.1} \tag{6.7}$$

From the equation of continuity, we have that:

$$c_{m1} \cdot A_1 = c_{m2} \cdot A_2 \tag{6.8}$$

The inlet diameter is fixed from Equation 6.5, so the blade thickness will only affect the runner inlet height, B_1. Equation 6.9 calculates the inlet height.

$$B_1 = \frac{A_1}{\pi \cdot D_1 - z_b \cdot \frac{t_{le}}{sin\beta_1}} \tag{6.9}$$

Where β_1 is found from Equation 6.10, t_{le} is thickness leading edge and z_b is number of runner blades.

$$tan\beta_1 = \frac{c_{m1}}{u_1 - c_{u1}} \tag{6.10}$$

The only input parameter value that will be varied in this thesis is the inlet reduced peripheral velocity $\underline{u}_1$. Therefore, the outlet dimensions, the design speed of rotation and volume flow for BEP will stay the same, but the inlet dimensions and the shape of the runner blades will vary. The variation on the inlet is illustrated in Figure 5 with a two-dimensional velocity profile where $\underline{u}_{1,1}$= 0.72, $\underline{u}_{1,2}$ = 0.75 and $\underline{u}_{1,3}$ = 0.8.

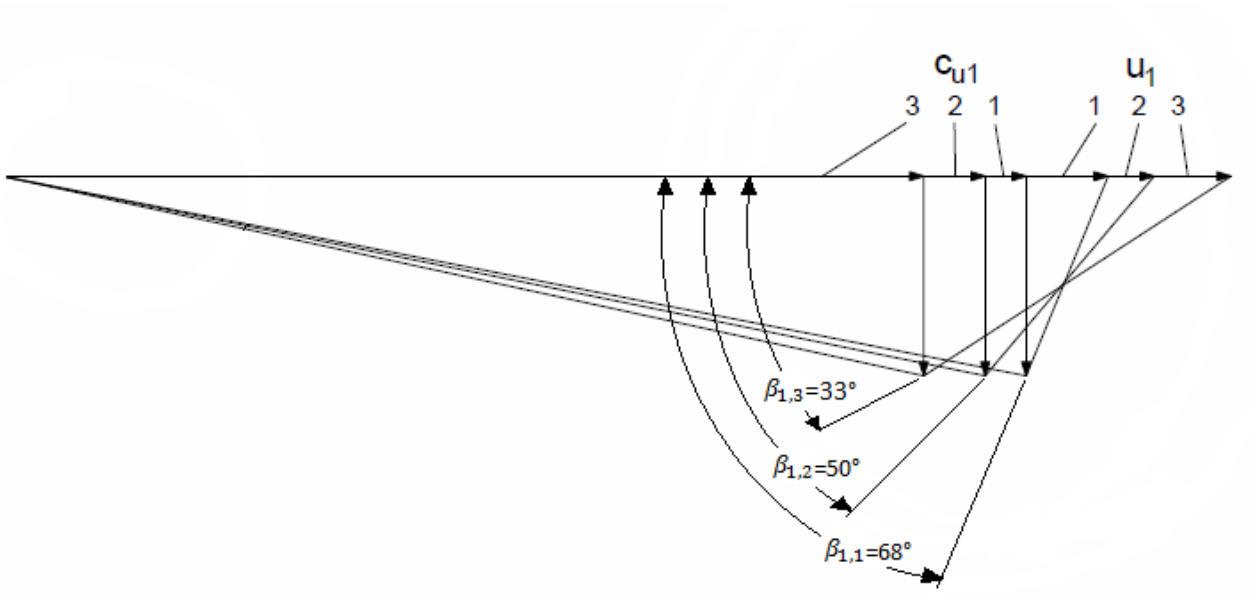

Figure 5 – Inlet velocity profiles at design point (BEP) for $\underline{u}_{1,1}$=0.72, $\underline{u}_{1,2}$=0.75 and $\underline{u}_{1,3}$=0.8.

The absolute velocity in the peripheral direction, c_{u1}, and the runner inlet angle, β_1, decreases when $\underline{u}_1$ is increased. The inlet diameter D_1 increases along with an increase in $\underline{u}_1$. Based on Equation 6.9 the inlet height, B_1, will decrease with an increase in D_1. Figure 6-8 displays the different runner geometries created with variations in $\underline{u}_1$.

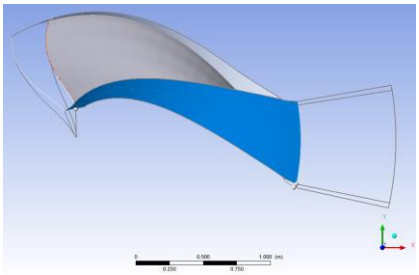

Figure 6 – Runner geometry when $\underline{u}_1$=0.72.

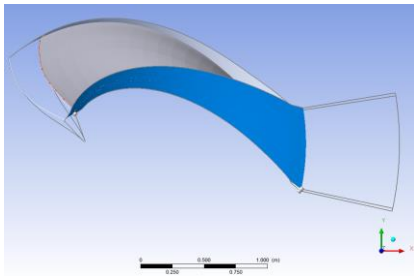

Figure 7 – Runner geometry when $\underline{u}_1$=0.75

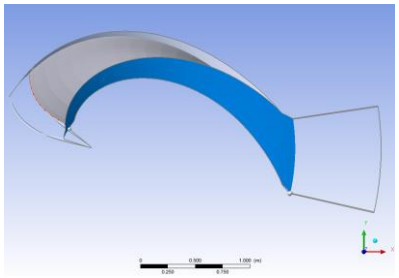

Figure 8 – Runner geometry when $\underline{u}_1$=0.8

An increase in $\underline{u}_1$ will also give a higher reaction ratio for the turbine. The reaction ratio is defined as the pressure fraction of the total net specific energy which is converted to mechanical energy in the runner and is given by Equation 6.11 [18]

$$R = \underline{c}_{u1}^2 \cdot \left(2 \cdot \frac{\underline{u}_1}{\underline{c}_{u1}} - 1\right) \tag{6.11}$$

Erik Os Tengs have connected Khoj to ANSYS Workbench during his doctorate. His setup creates the inlet area, runner blade and part of the draft tube for one runner blade in the turbine. There are 15 activated input parameters within the blade design stage, displayed in Table 1. These parameters can be altered with and adjusted to optimize a specific design. A lot of the initial design inputs have already been discussed earlier in this chapter.

Table 1- Input parameters for initial blade design

Parameter name	**Description**	**Initial design inputs**	**Unit**
Q	Volume flow	31	[m^3/s]
H	Nominal head	377	[m]
u_2	Outlet peripheral velocity	38	[m/s]
β_2	Outlet blade angle	19	[°]
acc	Acceleration from inlet to outlet	1.1	[2]
t_te	Thickness trailing edge	10	[6]
t_le	Thickness leading edge	20	[6]
z_b	Number of runner blades	17	[2]
$\underline{u}_1$	Inlet reduced peripheral velocity	0.72	[2]
b_ellipse	The shroud has an elliptic form, b says something about the size	0.69	[?]
ns	Numerical parameter, recommended >20 [7]	40	[2]
div	Numerical parameter, recommended >20 [7]	40	[2]
a_ss	Ellipse form leading edge suction side	30	[6]
a_ps	Ellipse form leading edge pressure side	10	[6]
GV	Guide vanes, 1= Yes, 0= No.	0	[2]

The initial design inputs are determined in collaboration with co-supervisor Ole Gunnar Dalhaug, a professor at the water laboratory [16]. According to Dalhaug, this is the closest approximation to the Tokke prototype for this turbine design software. Volume flow and nominal head are approximately the same as the prototype even though the head can vary to some extent at the site where the prototype is located. Both the Tokke prototype and model in the laboratory have 15 full runner blades and 15 splitter blades which give 30 blades at the inlet and only 15 at the outlet. This design model is created with full runner blades and no splitter blades. A runner with 30 blades at both inlet and outlet would be difficult or even impossible to weld. Dalhaug, therefore, suggested a design using 17 full runner blades. The output parameters needed to create a hill diagram is calculated by Khoj. The initial design outputs are displayed in Table 2.

Table 2 – Output parameters from blade design

Parameter name	Description	Initial design outputs	Unit
D_2	Outlet diameter	1.8006	[m]
Blades	Number of runner blades	17	[2]
Alpha	Guide vane angle	8.0912	[°]
RPM	Revolutions per minute	375	[2]

Within the constraints of the input parameters, the profile of one blade of the runner is created and exported back to ANSYS workbench where 3D coordinates of the blade component are obtained. The coordinates for the Hub, shroud, part of the draft tube and an inflow area are also created. The design is not a complete design of the turbine. Only the guide vane area, the runner area and part of the draft tube are created.

To only generate one blade and let the software copy the results around to emulate the whole rotating and stationary assembly, is a technique used for saving time and computational resources when simulating. This technique is often not possible to do because of different pitch between the components since number of guide vanes are uneven with the number of runner blades. However, this design does not create the guide vanes, and the different pitch will not create problems. The main reason the guide vanes are not generated in this simulation setup is because it would require new meshes for every guide vane angle which would be time-consuming.

If the same mesh had been used for all the different guide vane openings, the simulations would have to be run by a transient solver instead of steady state and twist the mesh for each alpha. The reason the spiral casing and full draft tube is not created is also done to save computational time. Furthermore, the splitter blades are not created either for simplicity reasons and because Khoj is not equipped with this feature. Figure 9 shows the creation of one runner blade including inlet and part of the draft tube. Figure 10 shows the completely emulated turbine.

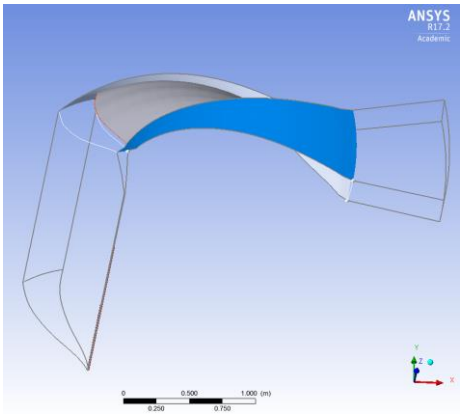

Figure 9 – one runner blade

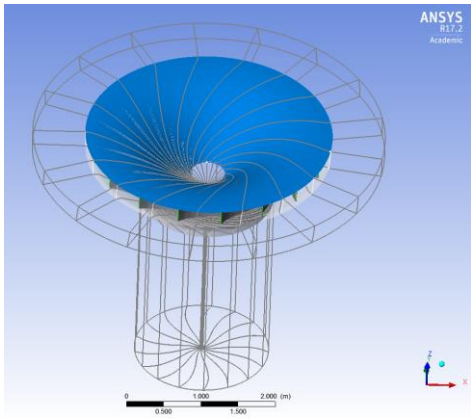

Figure 10 – Assembly of all 17 runner blades

6.2 Meshing software: ANSYS TurboGrid

A good mesh is essential to achieve reliable results. According to ANSYS TurboGrid automatically produces high-quality hexahedral meshes needed for blade passages in rotating machinery. The mesh created in TurboGrid is a structured mesh consisting hexahedral cells. Structured meshes give the quality and control to generate precisely the mesh necessary and are widely acknowledged to be superior to unstructured meshes [19].

In general, there are several advantages in using a structured mesh over an unstructured one. According to Chawner (2013), Hexahedron cell fills the same volume as tetrahedron cells with a fewer amount of cells thereby lowering both CPU time and memory. Also high-quality cells are easily generated on a hex grid with high aspect ratio, and the CFD solver converges better and produce more accurate results when the mesh is aligned with the predominant flow direction, which is the case for structured meshes as the mesh lines follow the curve of the geometry.

Another meshing strategy TurboGrid utilizes is a better mesh refinement in regions of interest for example close to the runner blade. In regions further away, that only represents geometry and transmitting load the mesh refinement is considerably lower. Elements in regions of less interest like the draft tube can be much larger, and thus the mesh is more rapidly created. A visualization of this can be viewed in Figure 11, and Figure 12 where it is seen that the cells become bigger and more stretched further away from the blade.

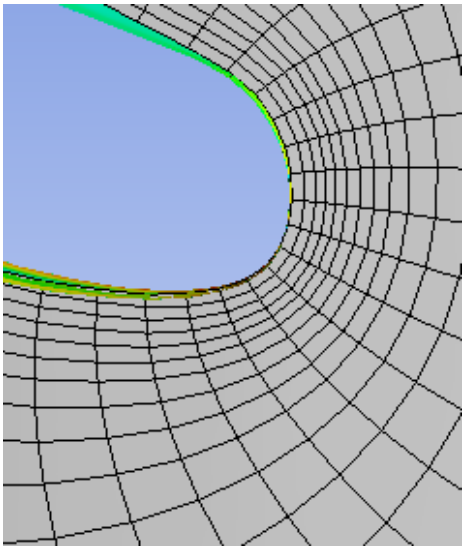

Figure 11 - Mesh at leading edge

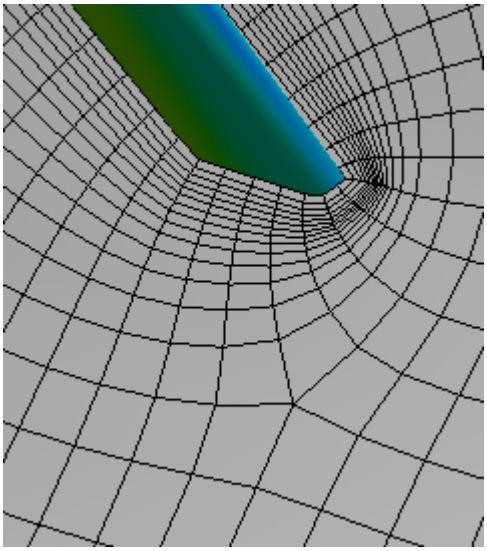

Figure 12 - Mesh at trailing edge

The turbine was divided into three domains: the inflow section, runner blade and draft tube. The mesh was independently created in all domains and connected with 2 interfaces. Figure 13 shows the hexahedral mesh with approximately 310.000 nodes for the whole section including approximately 265.000 nodes for the runner. These numbers vary with some extent for every design created.

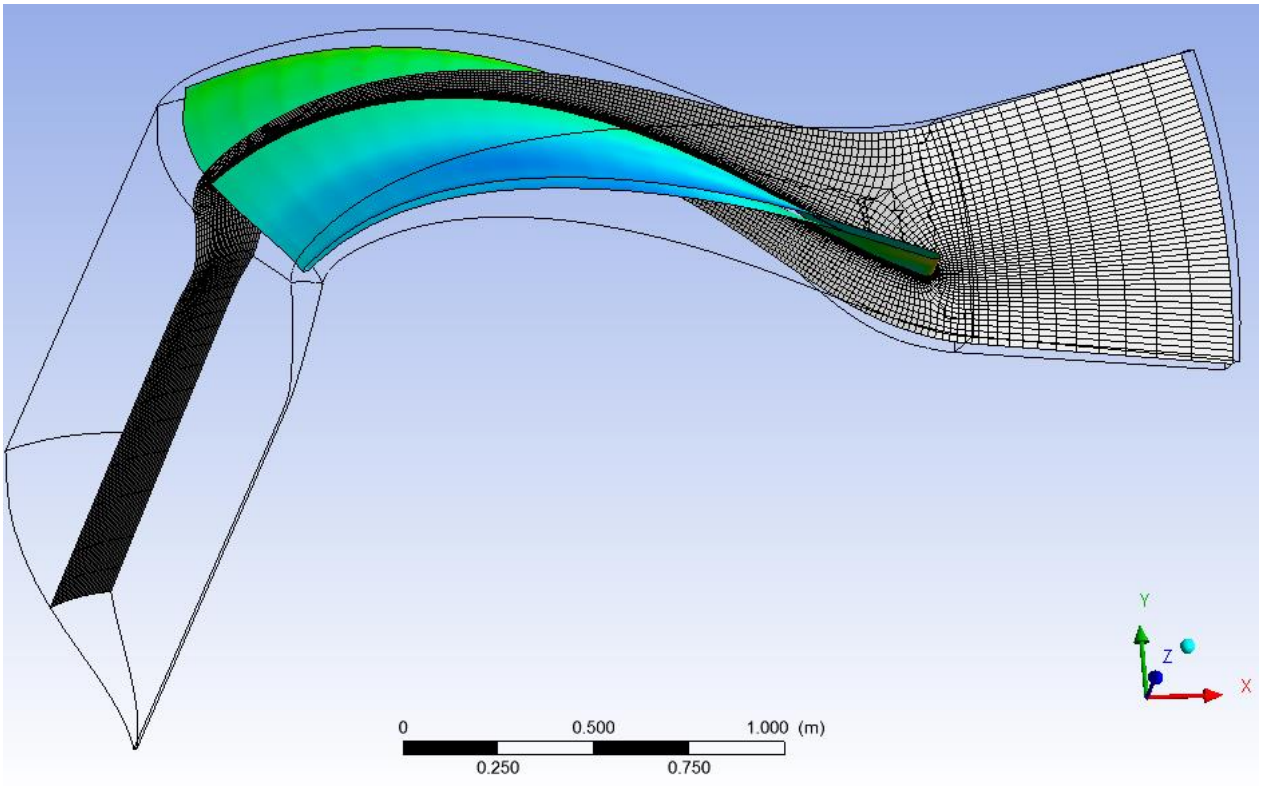

Figure 13 - Hexahedral mesh for the whole section

6.2.1 Mesh independence test

In TurboGrid one can choose between three embedded grid sizes; coarse, medium and fine or specify and exact grid size value. Figure 14-16 shows the refinement differences between the three embedded meshes.

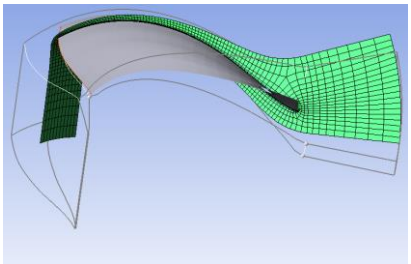

Figure 14 - Coarse grid size with approximately 20.000 elements

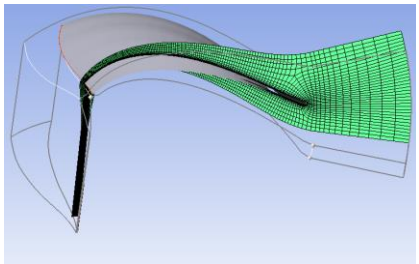

Figure 15 - Medium grid size with approximately 100.000 nodes

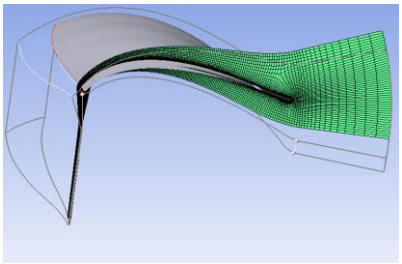

Figure 16 - Fine size grid with approximately 250.000 nodes

A mesh independence test is conducted to decide an appropriate mesh size. This is done to ensure that the results of the analysis are not affected by changing the size of the mesh. The number of nodes is plotted in against important global output values like head, mass flow, and hydraulic efficiency. The resulting plots can be viewed in Figure 17-19. The initial design described in Chapter 6.1 was used to conduct the mesh independence test. The input and output parameters for this design as well at the numerical setup can be found in Appendix C. It is chosen to test seven different mesh sizes in the range of approximately 20.000 nodes up to about 800.000 nodes.

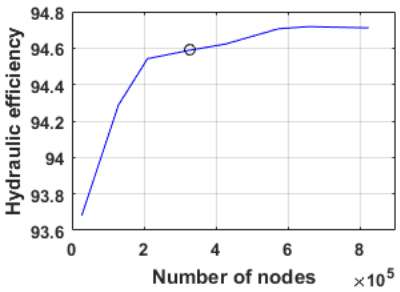

Figure 17– Hydraulic efficiency plotted against number of nodes

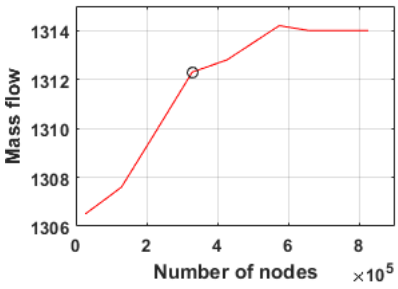

Figure 18– Mass flow through one runner blade plotted against number of nodes

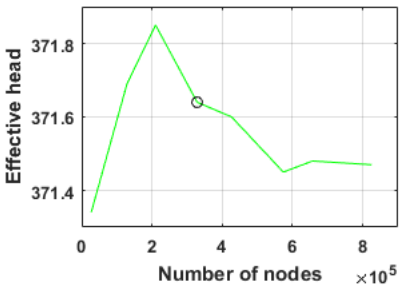

Figure 19 – Effective head plotted against number of nodes

In addition to the grid convergence test for the three global outlet parameters, the computational time has to be taken into consideration. The mesh independence test is only executed for a single point in the hill diagram and the simulations are done on a two core computer with 16 GB RAM and a maximum speed of 3.33 GHz. It was chosen to use mesh number 4, which had approximately 330.000 nodes including 275.000 nodes in the runner area. Deviation from the finest mesh tested were 0.13% for hydraulic efficiency, 0.13% for mass flow and -0.04% for the effective head. These deviations are considered acceptable for this purpose.

6.2.2 Mesh quality

Mesh limits in ANSYS defines the acceptable values for the mesh analysis variables. If the mesh is not created within these limits, TurboGrid highlights the problem areas of the mesh in mesh analysis and statistics. The different mesh limits with initial mesh limits are listed below in Table 3. These include maximum face angle, minimum face angle, connectivity number, element volume ratio, minimum volume and edge length ratio.

Table 3 – Initial Mesh limits

Measure	Limits type	Max/Min Value	Initial value	% Bad
Maximum Face Angle	Maximum	165 [degree]	145.76	0
Minimum Face Angle	Minimum	15 [degree]	34.75	0
Connectivity Number	Maximum	12	10	0
Element Volume Ratio	Maximum	20	5.92	0
Minimum Volume	Minimum	0 [m^3]	2.82e-10	0
Edge Length Ratio	Maximum	1000	2062.12	0.1034

ANSYS CFX solver guide recommends an aspect ratio less than 10.000, the minimum angle of element greater than 20 degrees, and a volume expansion lower than 10 [20]. This mesh is within all the recommendations from ANSYS even though the edge length ratio is a bit high. The reason for this is due to the long cells created in the draft tube and is not a big concern in these simulations. The problematic cells are highlighted in Figure 20. The setup information about the mesh independence test can be found in Table 5.

In the ANSYS result output file orthogonal angle, expansion factor and aspect ratio are considered as either good, acceptable or poor. Good is annotated with 'OK', acceptable with 'ok' and poor with '!'. The minimum or maximum value is presented for the different measures including the percentage distribution of good, acceptable or poor within the domain.

The mesh quality thresholds that define good (OK), acceptable (ok) and poor (!) are listed in Table 4.

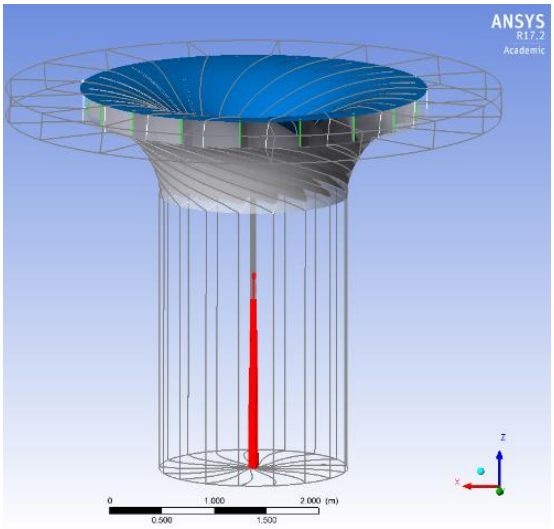

Figure 20 - Assembly of all 17 runner blades. Long cells in draft tube are highlighted in red.

Table 4 – Mesh quality thresholds[1]

Maximum aspect ratio	OK	<10000
	ok	10000<100000
	!	>100000
Maximum mesh expansion factor	OK	<5
	ok	5<20
	!	>20
Minimum orthogonal angle	OK	>50°
	ok	50°>20°
	!	<20°

6.3 Simulation solver: ANSYS CFX 17.2

6.3.1 CFX-Pre

CFX-Pre is where physical and chemical phenomena to be used in the simulation are selected. In addition, one defines the fluid properties and specify boundary conditions at the domain boundary. The mode of operation in CFX-Pre for this thesis is always set to be *Turbomachinery Mode.* This mode ensures a quick setup as the boundary conditions and interfaces between the components are automatically generated. The three domains can be seen in Figure 21-23.

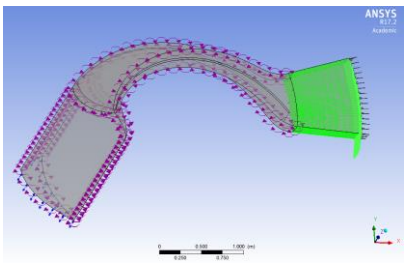

Figure 21– Domain 1: Inflow, stationary

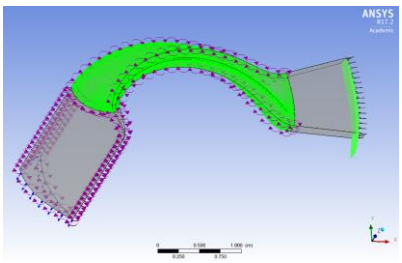

Figure 22 – Domain 2: Runner, rotating

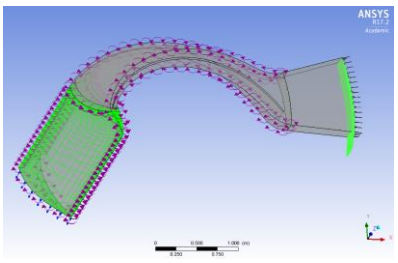

Figure 23 – Domain 3: Draft tube, stationary

The stationary inflow domain is created without guide vanes for simplicity reasons as explained in Chapter 6.1. The vaneless space=a is multiplied with 20 to get an extension of the vaneless space. The runner inlet angle is the same as the guide vane outlet angle. This assumption comes from free vortex theory [21] where $c_m r$ = constant and from the velocity triangles $c_m r = r c_u \tan \alpha$ which yields α=atan(c_m/c_u). Alpha is therefore constant in the inlet vane less space. This assumption is normal practice in vaneless spaces in turbine design [22].

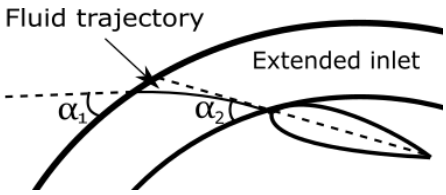

Figure 24- Fluid trajectory in Inflow vane less space[2]

The boundary conditions for the walls are chosen to be No Slip wall with a smooth surface with one exception. The draft cone is set to be free slip. TurboGrid does not prefer to make something that goes towards radius equal to zero. The inside of the hub is therefor set to almost reach zero but not become zero. This will lead to construction of a cone in the middle of the draft tube with a very small radius. For now this will have to be accepted so TurboGrid fast can create the mesh for the entire domain. Since there is only a small amount of flow that passes this cone. Free slip is therefore set to accept that the cone is present and not have any friction in the cone and to minimize the effect of its existence. Figure 25 shows the placement of the walls in the simulation model.

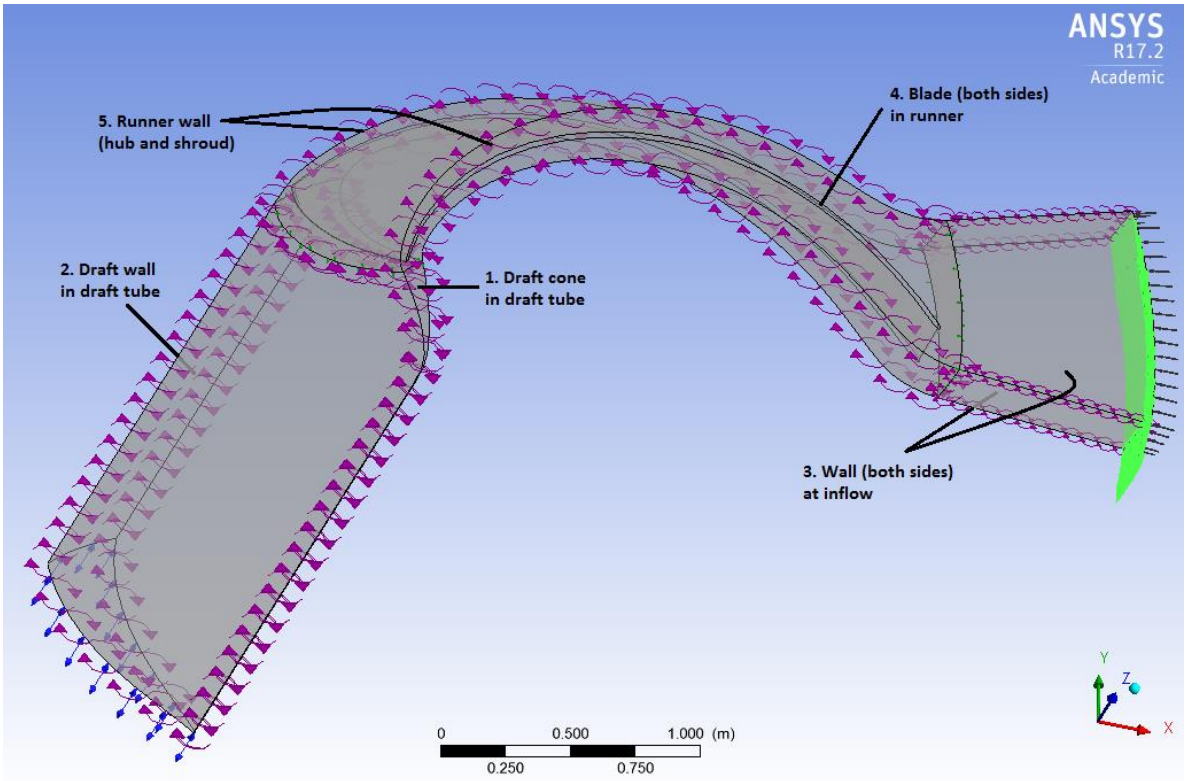

Figure 25 – Placement of walls in simulation model

The inlet boundary condition was defined as simple homogenous velocity profile with parameters presented in the Summary CFX transformation method run definition in Table 5. When simulating a new geometry the inlet velocity profile is not available, and this is done to have as realistic conditions as possible.

Outlet boundary condition was set to be opening, allowing flow in both directions, with a pressure of 0 Pa. The velocity direction is normal to the boundary condition. This was done for numerical stability of the simulation.

All the interfaces are shown in **Error! Reference source not found.** and include draft periodic interface side 1 and 2, runner periodic interface side 1 and 2, inflow periodic interface side 1 and 2, runner/draft interface side 1 and 2 and runner/inlet interface side 1 and 2. Conservative Interface Flux are chosen as the boundary condition for all interfaces.

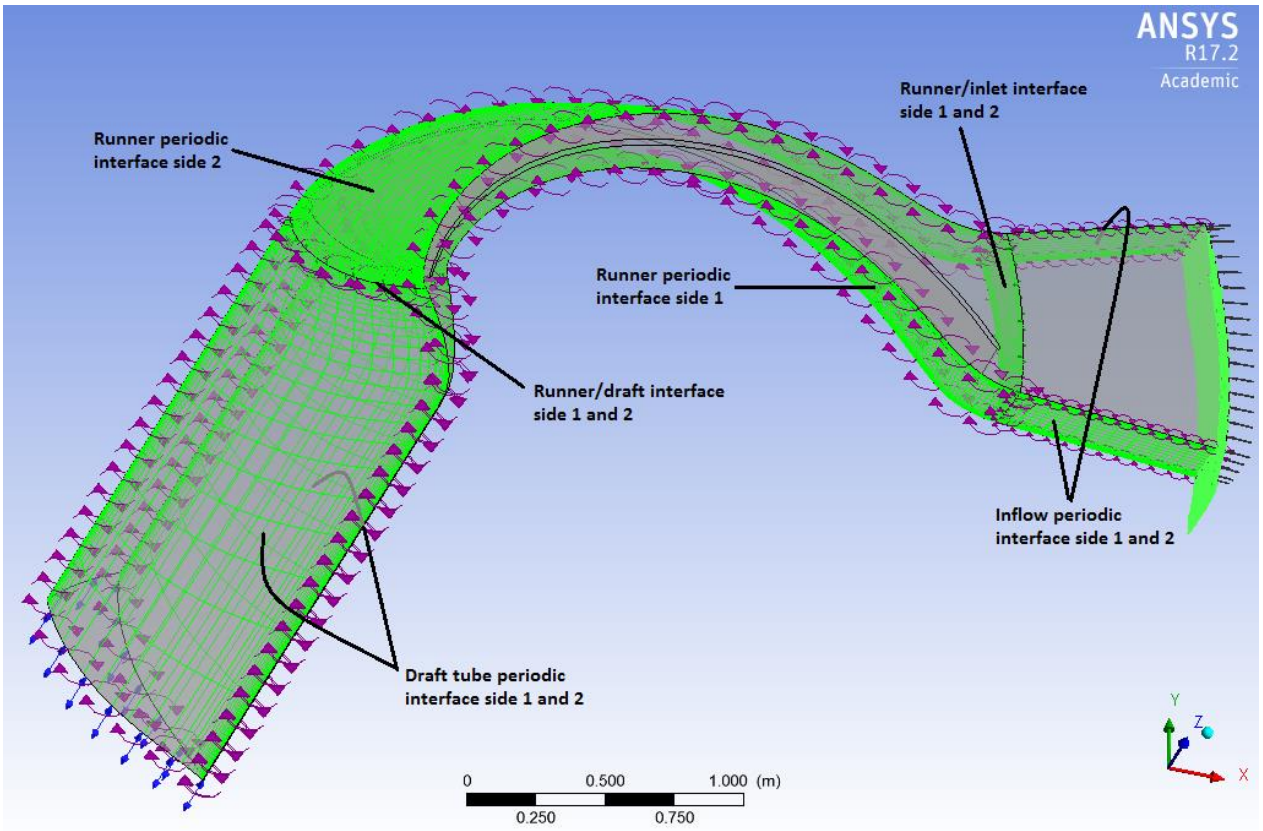

Figure 26 – Location of interfaces in simulation model

6.3.2 Solver

The set of equations solved by CFX is the unsteady Navier-Stokes equations in their conservative form for mass, momentum, and energy. The set of Navier-Stokes equations and more information on solver theory can be found in Appendix E. CFX uses the finite volume technique. The region of interest are divided into small sub-regions called control volumes. The equations are discretized and solved iteratively for each control volume. The partial differential equations are integrated over all the control volumes which are equivalent to applying a conservation law to each control volume. As the solution approaches the exact solution, it is said to converge. Another important feature of ANSYS CFX is its use of a coupled solver, in which all the hydrodynamic equations are solved in a single system. The coupled solver is faster than the traditionally segregated solver, and fewer iterations are required to obtain a converged flow solution [23].

Turbulence model

The SST turbulence model is a two equation Eddy viscosity model that combines to widely used turbulence models, k- ω and k-ε. The k-ω is used from the wall to the viscous sublayer, and the k-ε is used for the free stream. Menter first created the BSL model which combines the advantages of the Wilcox and the k-ε model but still fails to properly predict the onset and amount of flow separation from smooth surfaces. The reason for this deficiency is given in Menter [24].

The main reason is that neither of the models accounts for the transport of turbulent shear stress which results in an over-prediction of the eddy-viscosity. Menter, therefore, created the SST model where he modified the definition of the eddy viscosity to account for the transport of the principal turbulent shear stress. The full set of equations utilized in the SST turbulence model can be found in Appendix E.

Two-equation turbulence models are very widely used as they offer a good compromise between numerical effort and computational accuracy according to SHARCNET. Both the velocity and the length scale are solved using separate transport equations (hence the term 'two equation'). The k-ω based SST model accounts for the transport of the turbulent shear stress and gives highly accurate predictions of the onset and the amount of flow separation under adverse pressure gradients [25].

Two equation models that incorporate the eddy-viscosity concept suffer from the following drawbacks: (1) they are not able to properly account for streamline curvature, rotational strains, and other body-force effects; (2) they neglect nonlocal and history effects on Reynolds-stress anisotropies [26]. According to Holo [27] the SST-turbulence model fails to calculate the turbulence in the surrounding areas of the stagnation points. Simulations conducted by Trivedi in connection with the Francis-99 project shows that both the k-ε and SST turbulence model worked well [28]. However, these simulations were transient and not steady state. Gavrilov et al. [29] tried k-ω, SST, ζ-f and RSM. The Reynolds stress models calculate the same torque, and the pressure distributions on the runner blades with small variations. They also demonstrate the same results near the leading edges of the blade but differ in the area around the trailing edges. Based on this as well as recommendations from more experienced ANSYS users like Erik Os Tengs and Chirag Trivedi SST is chosen as the applied turbulence model.

Calculation of global output values

To make the simulation as similar to the experimental setup in the laboratory the following equations are defined in ANSYS to calculate torque, head, pressure, mass flow and efficiency.

$$\tau_{tot} = \tau_{blade} + \tau_{runner\ wall} \tag{6.12}$$

$$H = \frac{p_{tot1} - p_{tot2}}{\rho g} \tag{6.13}$$

Where p_{tot} is defined as the pressure that would exisit at these points if the fluid was brought instantaneously to rest. For incompressible fluids, such as water, the total pressure is given by Bernoulli's equation.

$$p_{tot} = p_{stat} + \frac{1}{2}\rho(U \cdot U) \tag{6.14}$$

Which is the sum of the static and dynamic pressures. U is the velocity vector $U_{x,y,z}$.

$$\omega = \frac{2\pi n}{60} \tag{6.15}$$

Where n is rotational speed in [rev/min]. Hydraulic efficiency is calculated with equation 6.16.

$$\eta_h = \frac{\tau_{tot}\omega}{\rho g H Q} \tag{6.16}$$

When inserting for head (H) and volume flow (Q) we get:

$$\eta_h = \frac{T\omega}{(P_{tot1} - P_{tot2}) \cdot \frac{m_1}{\rho}} \tag{6.17}$$

6.3.3 CFX-Post

CFX-Post is where the results are extracted and allows the user to review the results visually and graphically, and different parameters can be studied.

6.4 Setup summary

Table 5 give a summary of the setup, used in all the simulations, including information on the mesh, interfaces, boundary conditions, fluid properties, solver and convergence control, turbulence model and computer capacity and speed.

Table 5 – CFX transformation method run definition

Parameter	Description
Simulated components	**Domain 1:** Stationary, inflow without guide vane **Domain 2:** Rotating, runner blade **Domain 3:** Stationary, draft tube
Grid type	Multiblock, Hexahedral, approximately 310.000 nodes
Simulation type	Steady state
Interfaces	**Runner Periodic:** For duplication of blades: Rotational periodicity, Mesh connection: GGI **InflowPeriodic and DraftPeriodic:** Rotational Periodicity, Mesh connection: GGI **InflowRunner and RunnerDraft:** General connection, Frame Change/Mixing Model: Frozen rotor, Pitch Change: Automatic, Mesh connection: GGI
Boundary conditions	**Inlet**: Mass flow rate: Varies between 950-2400 kg/s depending on GV opening for each runner blade, 16.150-40.800 kg/s in total. Turbulence intensity 5% Flow Regime: Subsonic, Mass and momentum: Total pressure(stable), Relative pressure: NomHead*9.81*1000[Pa] Direction on cylindrical components: axial 0, Radial –Cm(=1), theta –Cu(=1) **Outlet**: Opening, pressure (0 Pa) and direction (normal to boundary condition), turbulence intensity 5% **Walls**: Smooth walls with no slip condition with exception of Draft cone with free slip
Fluid	Water at 5°C, Heat transfer: Isothermal
Solver control	Advection Scheme: High resolution
Convergence control	Min-max. Iterations (100-500), Physical timescale (-1/omega[s^-1]), residual target(RMS): 1E-5
Turbulence model	SST
Run type	2 cores (Intel(R) Core(TM) i5 CPU 660@ 3.33GHz) RAM 16 GB

7 Results and discussion

In this chapter, experimental and numerical results are presented. This includes a full run of the Tokke model in the laboratory. The speed of rotation is regulated in the range of ±20 % from BEP and guide vane opening, α, is regulated in the range of ±40% from BEP. Two simulations of the prototype are also presented.

It is assumed that the first simulation corresponds best with the prototype at Tokke where $\underline{u}_1$ is set to be 0.72. This simulation design is further referred to as design 1. In the second simulation, $\underline{u}_1$ is changed to 0.8, which changes the runner geometry as well as turbine inlet dimensions. This simulation design is further referred to as design 2. Only 56 points in the hill diagram are simulated for design 1 and 2.

It was desired to conduct simulations on more than two designs. However, due to time restraints, only two designs were evaluated. The simulations had to be run several times over due to mistakes discovered after the simulations were conducted.

7.1 Experimental results from Tokke model in the hydropower laboratory at NTNU

Postdoctoral researcher Chirag Trivedi (*chirag.trivedi@ntnu.no*) have provided one of the datasets from the experimental study from the first Francis-99 workshop held in December 2014 at NTNU. The dataset provided nine different guide vane angles and fifteen different speed numbers for each guide vane angle.

A hill diagram is created in MATLAB following the procedure presented in Chapter 6. This is illustrated in Figure 27. The maximum efficiency of 93.2 % was observed at n_{ED}=0.1761 and Q_{ED}=0.1428. The total uncertainty in hydraulic efficiency was calculated to be ±0.16%. The full setup including all uncertainties can be found at NVKS research pages under Francis-99.

At a late stage in the of this project, it was noticed that the dataset provided by Trivedi was missing one guide vane angle, α=9.84. There was not enough time to include the guide vane angle and create the new hill chart. The hill chart presented in Figure 27 is therefore not equal to the hill chart found at NVKS research pages.

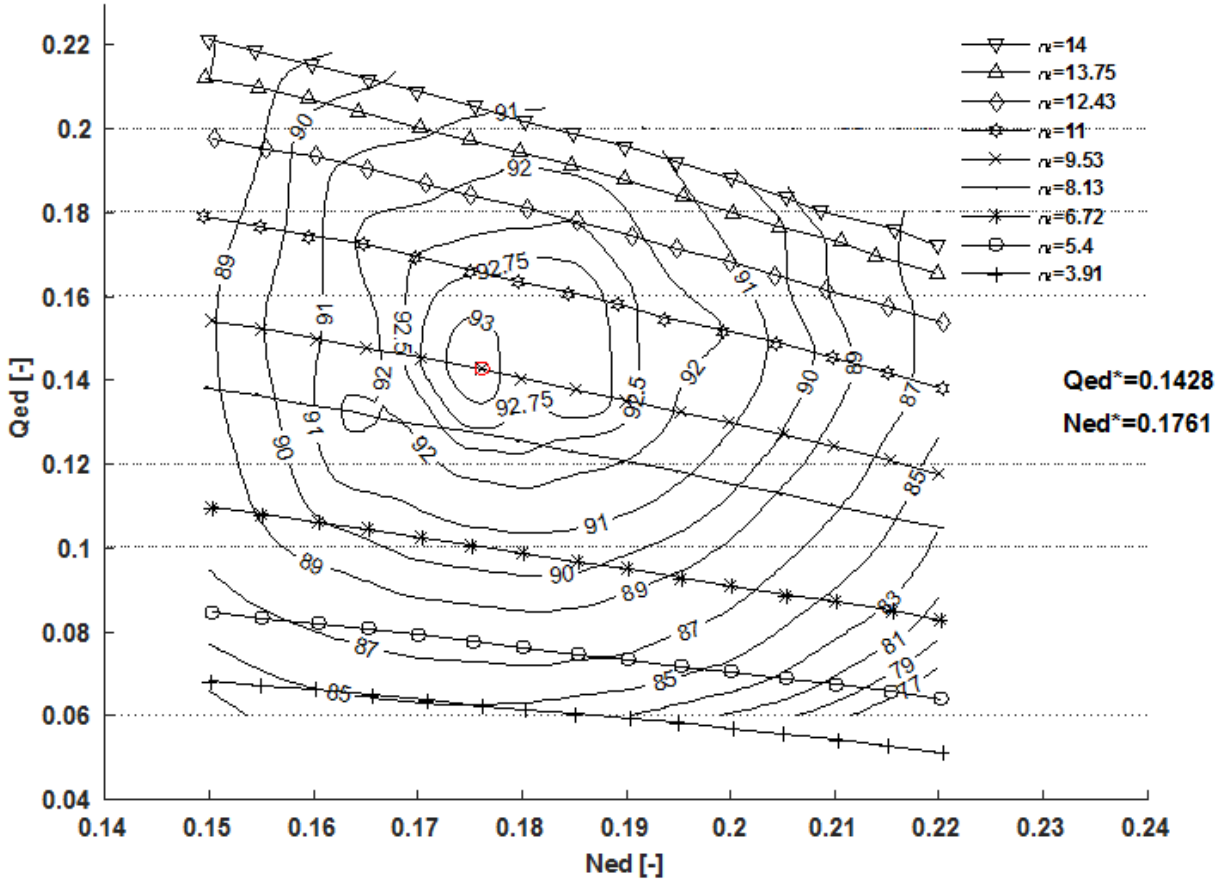

Figure 27 – Hill Diagram for Francis-99 experimental study conducted in December 2014

In Figure 28, a graph of efficiency plotted against the power output is visualized. The numbers are scaled up to match the Tokke prototype values. Hydraulic efficiency is multiplied with 1.0042 and, power output is calculated with Equation 7.1.

$$P_{prot} = \eta_h \cdot \rho \cdot g \cdot Q \cdot H_{prot} \qquad \text{[W]} \qquad (7.1)$$

It is chosen to plot seven different values of α close to BEP. For each α including all the different corresponding RPMs, efficiency is plotted against power output. One line for the values corresponding to RPM=375 is also plotted in Figure 28.

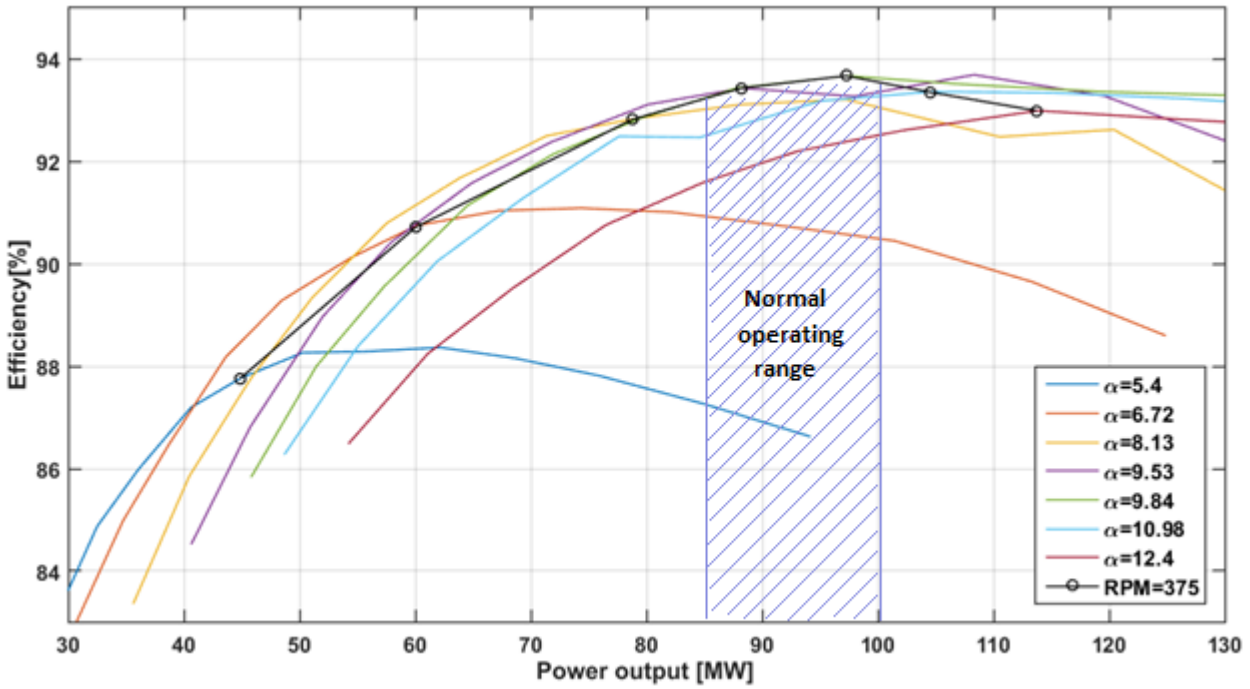

Figure 28 – Efficiency plotted against power output for 7 different guide vane angles including all the different corresponding RPM values

It is assumed that the prototype at Tokke would yield a similar result if it were run at different values for the rotational speed as the turbines are quite similar to each other. Tokke is normally operated between 85-100 MW, and it is noticed that within this range there would not have been much efficiency gain if the speed was adjusted since n = 375 has the highest efficiency in this range.

There are some design differences between the prototype at Tokke and the Tokke model in the lab. The model is designed by NTNU, and the prototype is designed by Andritz. The both have 28 guide vanes, 15 full runner blades and 15 splitter blades as well as the same speed number. The model is scaled down 1:5.1.

7.2 Numerical results of design 1, u_1=0.72

The design parameters chosen for design 1 is displayed in Table 1, which is presented in Chapter 6.1 and in Appendix C. The numerical setup that was applied can be viewed in Table 5 in Chapter 6.4. Guide vane angle, α, was chosen to be between 7-13 with a one-degree interval and the speed of rotation is set to be between 355-425 with an interval of 10. The hill diagram for this design is displayed in Figure 29. The maximum efficiency of 95.8 was observed at n_{ED}=0.202 and Q_{ED}=0.1627. BEP have an alpha of 13 and an RPM of 405.

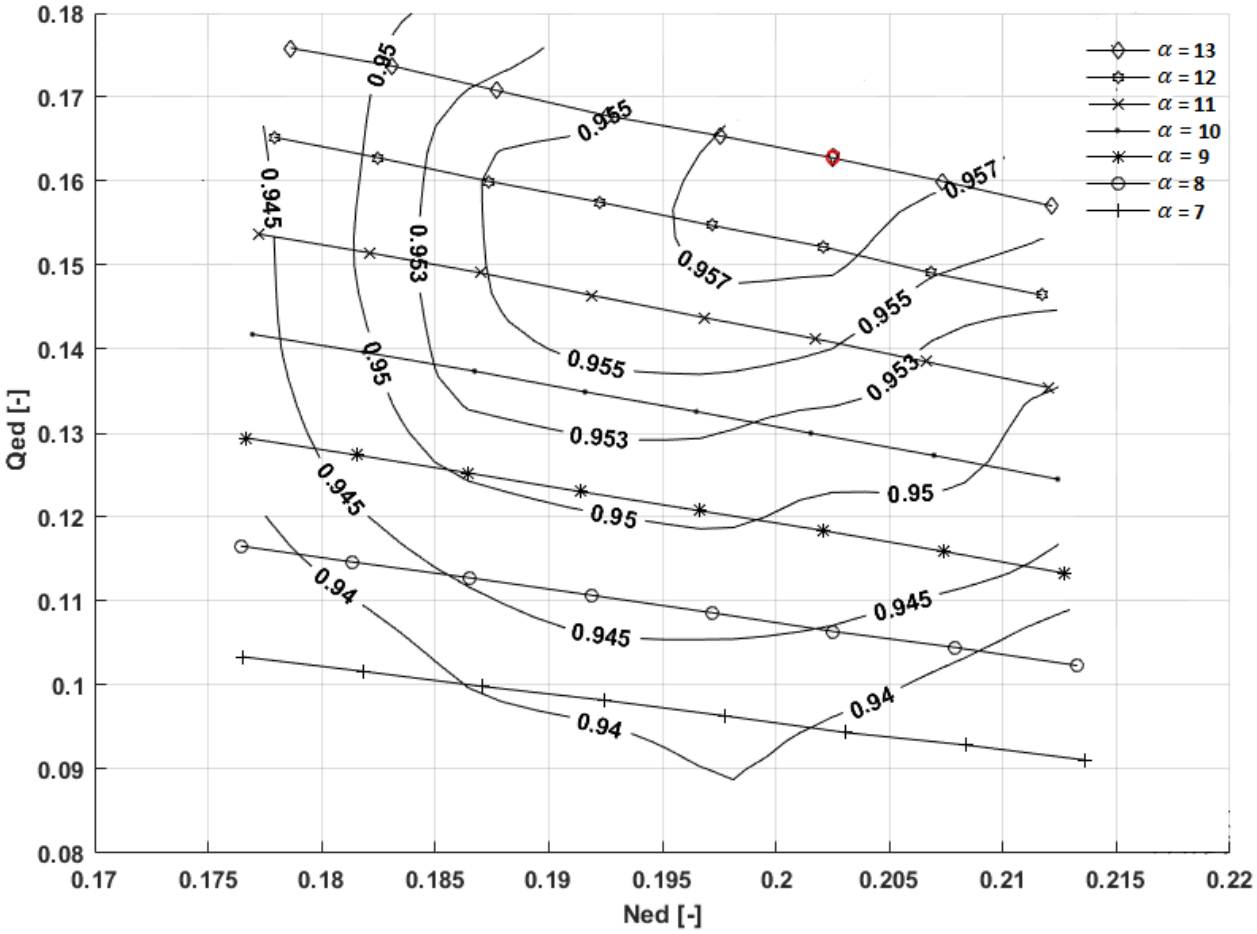

Figure 29 – Hill diagram for simulated design similar to the Tokke prototype where u_1 is set to be 0.72

Even though certain combinations of α and RPM were forced to stop at 500 iterations because it did not reach the residual target, most of the points converged after 350 iterations. The points that struggled to converge were points with low α-values and high n. It was also tried to simulate guide vane angle α=14. Most of the points failed to converge due to the setup restrictions regarding the alpha value, and these were therefore not included. The restriction was set to be 14.1°. This could be altered but was not done due to time restraints.

To get a sense of the uncertainty in the global output values, one point was observed in the solver monitor. This point chosen to monitor had α = 9 with an n of 375. The flow has an uncertainty of

0.12 %; head has an uncertainty of 0.02 % and the efficiency an uncertainty of 0.13%. Even though the uncertainty test is only done for one design point, most design points converged with similarly acceptable deviation. The mesh statistics for the different domains are considered to be either, good, acceptable or poor according to ANSYS. The Expansion factor is considered good for all the domains. The minimal orthogonal angle in the runner domain is 17% acceptable and 83 % good. The aspect ratio in the draft tube is considered 3% poor, 16% acceptable and 81% good. This is due to quite long cells in the draft tube as explained in chapter 6.2.2. If the mesh is considered as poor, it might indicate potential accuracy or convergence problems [31]. The procedure of calculating the uncertainty as well as the full mesh statistics for this design can be found in Appendix F.

Figure 30 and 31 shows the same areas of the hill diagram of the Tokke model and the hill diagram for design 1. It seems like neither BEP nor hill curves coincide well with each other. Efficiencies are in general higher for the simulated hill chart.

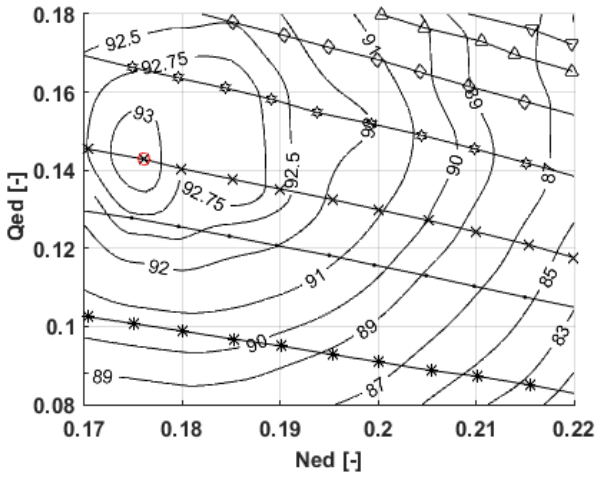

Figure 30 – An excerpt of the hill chart from the Tokke model

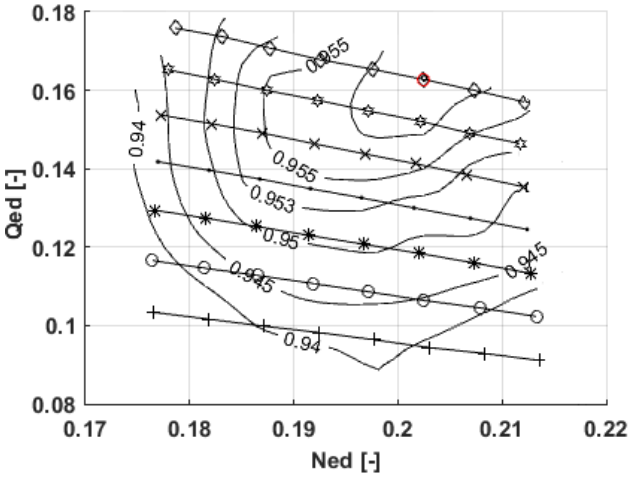

Figure 31 –Hill chart of design similar to the Tokke prototype, design 2

There are design differences between the experimental and numerical turbine. In the numerical design, the guide vanes, stay vanes and spiral casing does not exist. Only part of the draft tube is present, and there are no splitter blades, only regular full runner blades. In addition to this, there have been made many simplifications in the numerical setup. Only one seventeen of the turbine is simulated. Due to all these differences and the simplifications done in the numerical setup and solver control, it is not unreasonable that the hill diagrams look so different from each other. More time could have been spent on making the initial design more similar to the Tokke prototype.

For comparative reasons, Statkraft has provided data from a measurement of efficiency and power output conducted in 2012. The actual value of the efficiencies are confidential and is not possible to present in this thesis. The data have been normalized by dividing all the efficiencies with the highest efficiency, so BEP is located at a value of 1. Design 1 and the Tokke model has

also been normalized with their own BEP efficiencies. Figure 32 displays normalized efficiencies plotted against power output.

From the data received from Statkraft, it is not clear if the power output is the generator output or turbine output. Generator efficiencies are not included in the experimental Tokke model nor the prototype simulations. The power output of the model and prototype simulation are calculated with equation 7.1 including only hydraulic efficiency. The guide vane opening α is not known for the Tokke prototype, but the head is constant = 377 m. This is assumed to be the nominal head. For the model, the effective head is constant at approximately 370 m for n =375. Nominal head for the prototype simulation is set to be 377 m, and the effective head is approximately 370 m.

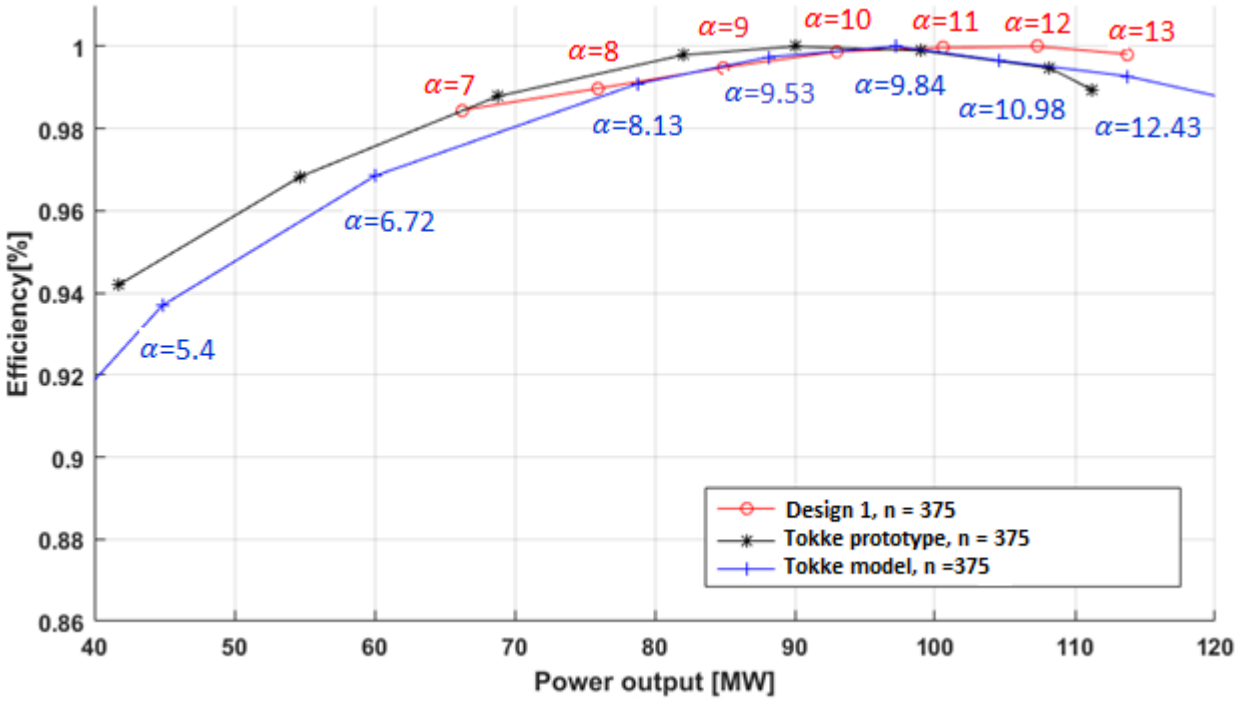

Figure 32 – Normalized efficiency plotted against power output for design 1, Tokke prototype and Tokke model. Only values for n = 375 are plotted.

From Figure 32 it comes forth that the normalized results yield similar shape even though the values are different.

Figure 33, the normalized numbers are converted back to their actual efficiency values, and the results of the measurements of the Tokke prototype is removed. Efficiency is plotted against power output for the design 1 and Tokke model. For design 1, efficiency and power output are also plotted for the different alpha values including n in the range of 355-425.

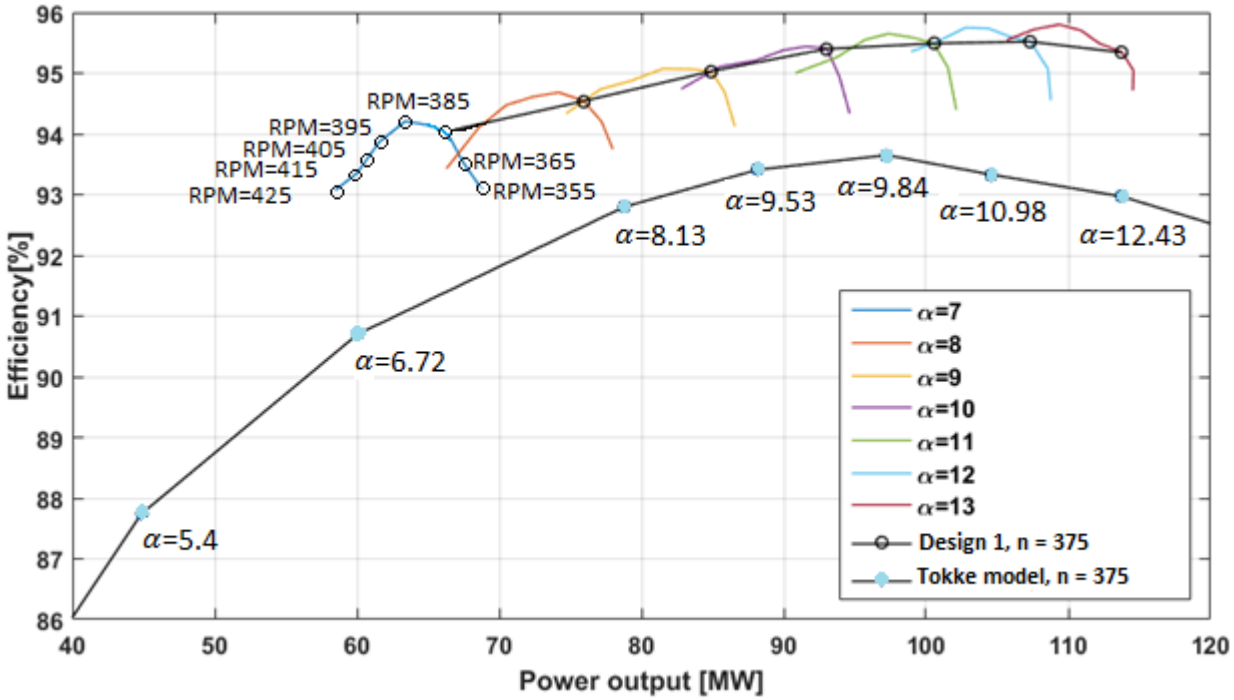

Figure 33 – Efficiency plotted against Power output for prototype simulation design where $\underline{u}_1$=0.72 and experimental results for the Tokke model. Efficiency against power is also plotted for all alpha values, consisting different values of n (355-425), of the prototype design.

For n = 375 the average deviation of efficiency between design 1 and experimental model is approximately 2.25%. This means that the simulation, on average, has an efficiency of 2.25 higher that the experimental results. For design 1, it seems there could be an efficiency gain of 0.25% for α = 12 and 13 if the variable speed could have been adjusted. However, a guide vane angle of 12 and 13 are not within the normal power operating range, which is between 85-100 MW. It looks like the maximum efficiency gain found within the normal operating area can be found at a power output of 97 MW. The speed would have to be adjusted to 395 rpm, and the efficiency gain would be at 0.2%.

The deviation might be explained by the previously mentioned simplifications in the numerical design and setup.

7.3 Numerical results of design 2, $\underline{u}_1$ = 0.80

The design parameters chosen for this design can be found in Appendix C. The numerical setup that was applied can be viewed in Table 5 in Chapter 6.4. Alpha is chosen to be between 7-13° with a one-degree interval and n is chosen between 355-425 with an interval of 10. The maximum efficiency of 95.9 was observed at n_{ED}=0.1965 and Q_{ED}=0.1326. At BEP α = 11 and n = 395.

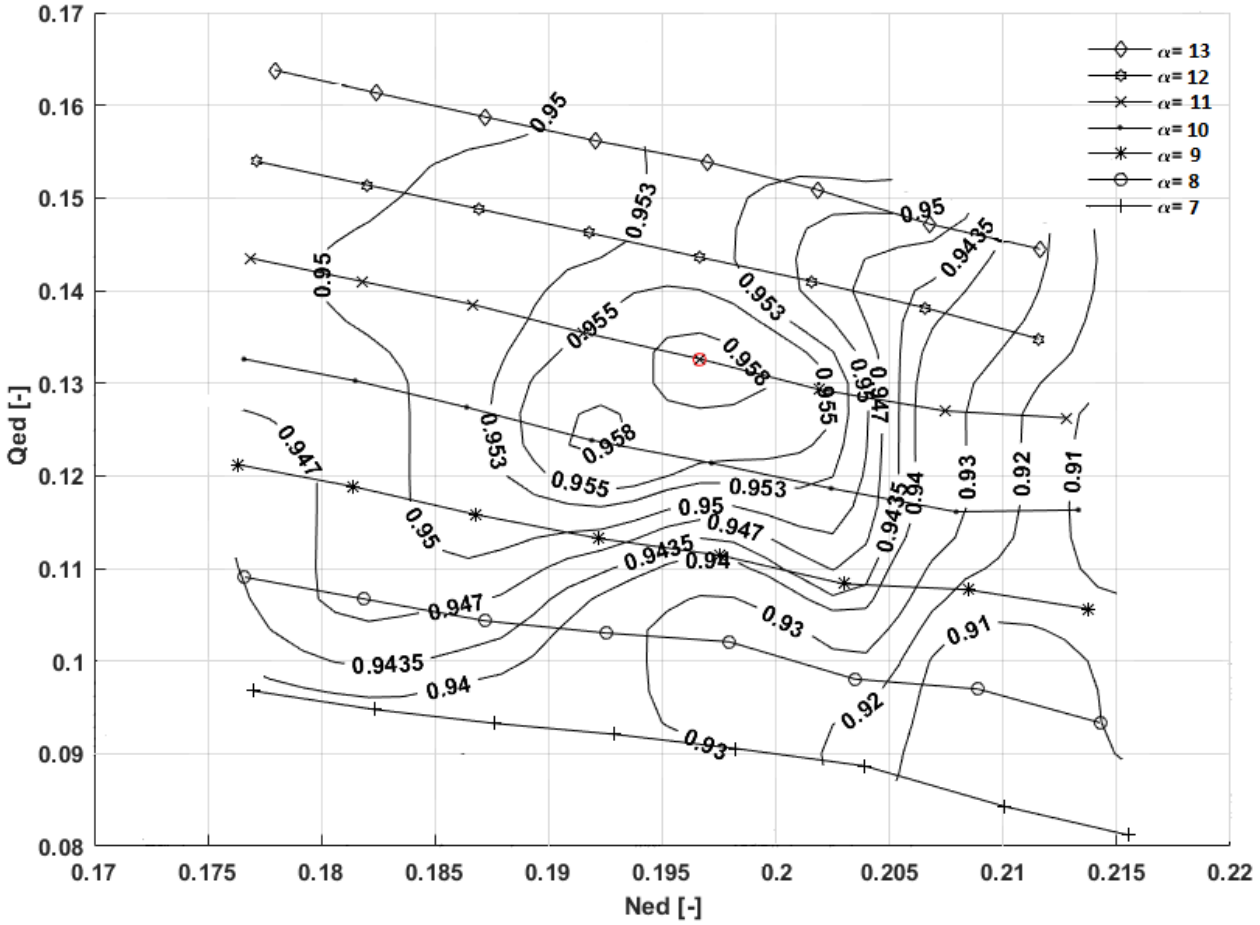

Figure 34 - Hill diagram for simulated design similar to the Tokke prototype where $\underline{u}_1$ is set to be 0.80, Design 2

Most results reached the residual target after around 400 iterations with some exceptions in regions away from BEP. To be able to say something about the uncertainty of the numerical results where $\underline{u}_1$ is 0.8, the flow, head, efficiency and residual targets for mass and momentum are observed for one point in time step monitors, same as for design 1. The run that was chosen to observe had α = 11 and n = 375. Even though the uncertainty test is only done for one design point, most design points converged with similarly acceptable deviation. The flow has an uncertainty of 0.44 %; head has an uncertainty of 0.06 % and the efficiency an uncertainty of 0.58%. It is unclear why the uncertainties for design 2 are 3-4 times higher than the uncertainty values for design 1. This mesh has the approximately the same mesh statistics as the previous

mesh. The methods used to calculate the uncertainty, as well as mesh statistics for design 2, can be found in Appendix F.

Figure 35 displays normalized efficiencies plotted against power output. The red lines show design 1 and the green line design 2. The black line shows the values of the Tokke prototype.

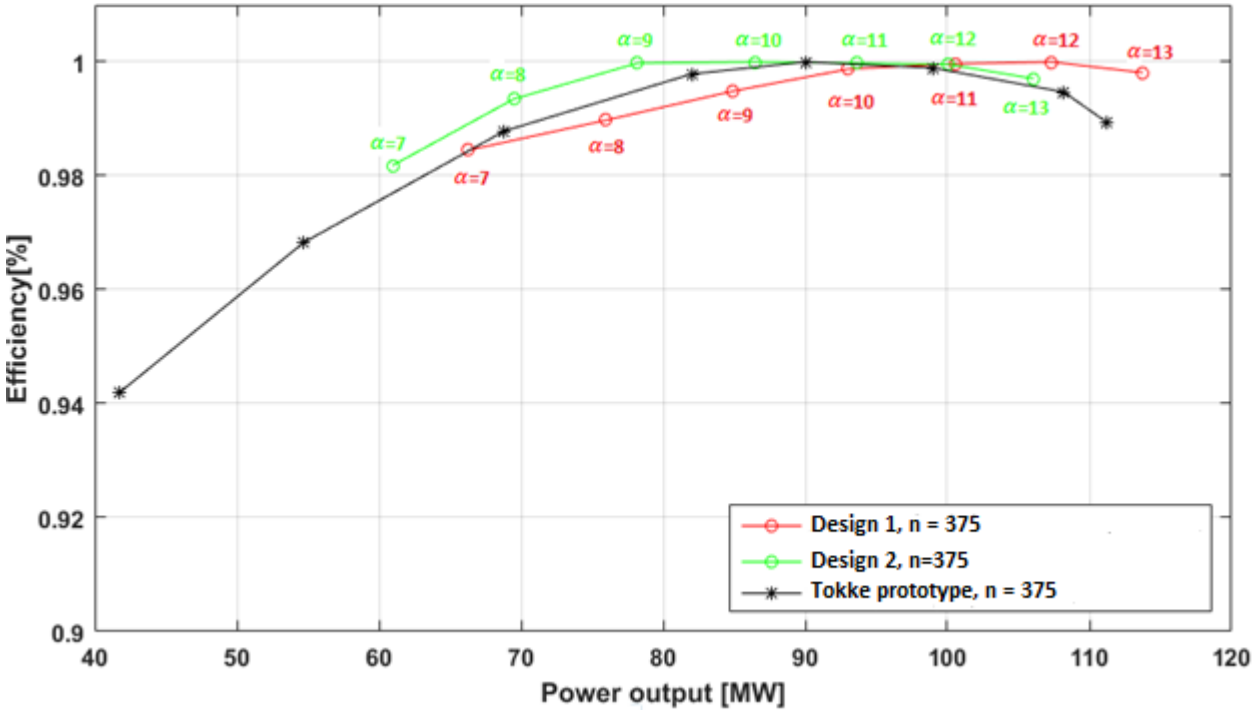

Figure 35 – Normalized efficiencies plotted against power output for prototype simulation $\underline{u}_1$=0.72, prototype simulation $\underline{u}_1$=0.8 and for the Tokke prototype. RPM is kept constant at 375. The red lines shows design 1 and the green line design 2. The black line shows the values of the Tokke prototype.

Figure 35 indicates that the efficiency curve for design 2 stays flatter a little longer on part load side than the efficiency curve for the Tokke prototype. On the high load side, design 2 coincides quite well with the prototype. This is the same trend as shown in Figure 3, Chapter 3.4, for the USBR pump turbine.

However, Figure 35 should not be reviewed alone since the actual efficiency values do not come forth in this display. If the values are not normalized and the Tokke prototype is excluded, the results will be the same as presented in Figure 36.

If the normalization of the values are removed, and the values of the Tokke prototype is excluded Figure 36 comes forth.

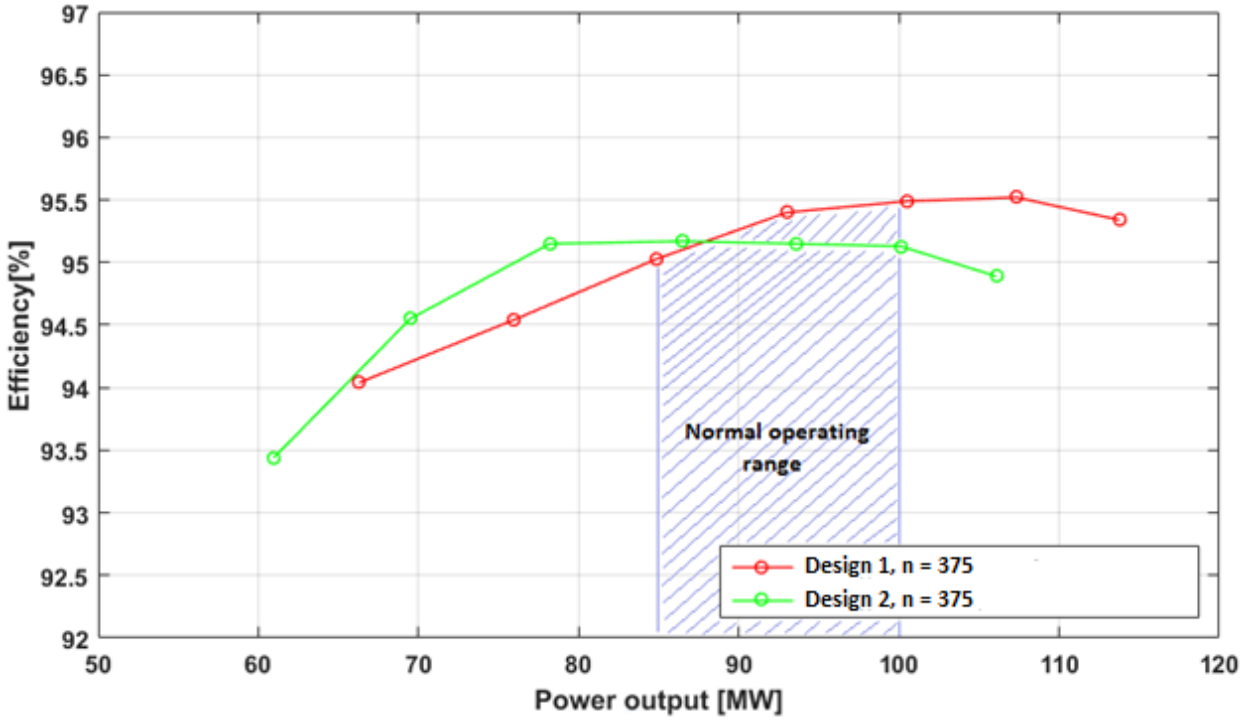

Figure 36 – Efficiency plotted against power output for prototype simulation where $\underline{u}_1$=0,72 and prototype simulation where $\underline{u}_1$=0.8.

Within the normal operation range at Tokke, the design 1 has the overall highest efficiencies. At part load, on the other hand, the design 2, has higher efficiencies. In the next figure α = 9-13, including n in the range 355-425, for the design 2 are included.

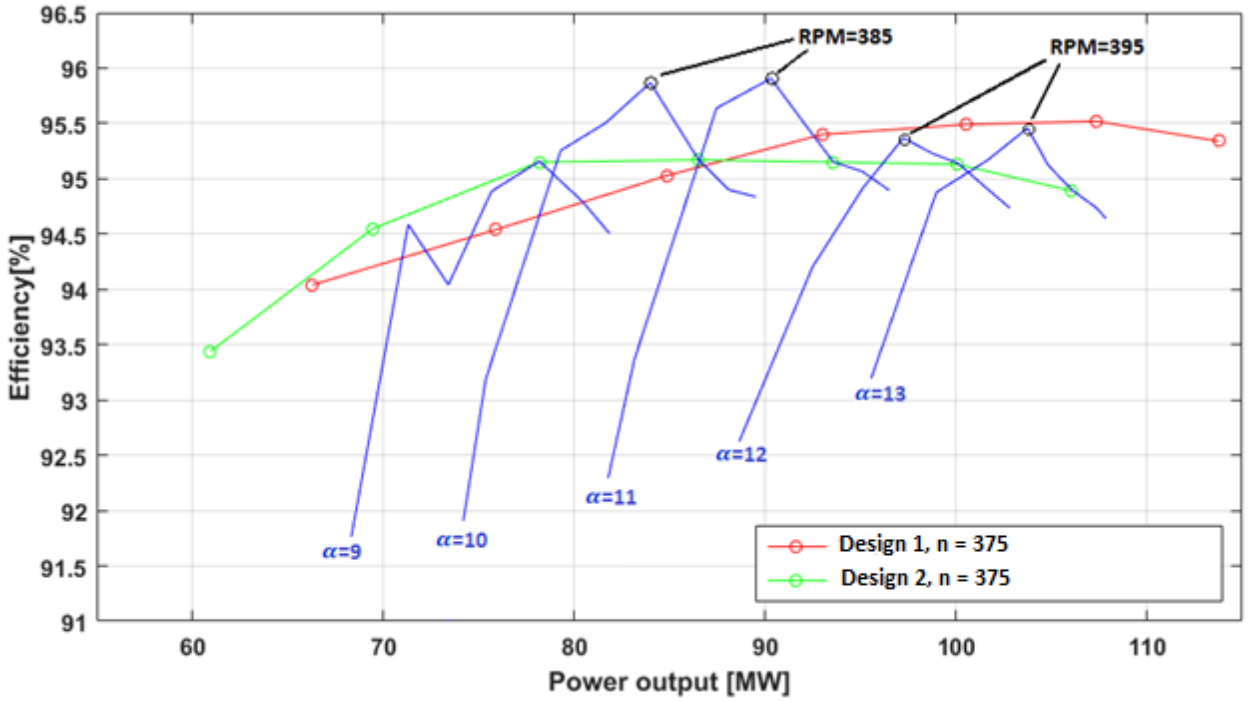

Figure 37 – Efficiency plotted against power output, at RPM=375, for prototype simulation where $\underline{u_1}$=0,72 and prototype simulation where $\underline{u_1}$=0.8. Five different alpha values, consisting of RPM in the range of 355-425, for the prototype simulation where $\underline{u_1}$=0.8, is also included.

If the speed is adjusted, for design 2, to 385 for α = 10 and 11, an efficiency gain of approximately 1.2% can, according to the results, be achieved. If the speed is adjusted to 395 for α = 12 and 13 efficiencies for design 2 can be increased very close to the same efficiencies as for design 1. This corresponds to an increase in efficiency, for design 2, of 0.5% and 1% respectively.

Even though the simulated prototype, design 1, does not correlates very good with experimental data, the simulations, which are conducted in the exact same manner relative to one another, shows a promising trend for variable speed operation.

8 Conclusion

The turbines at the Tokke power plant was selected for recreation and simulation in this thesis.

A design that resembles the prototype and model have been created and simulated. This design is referred to as design 1 in the thesis. The hill diagram obtained from this design have been compared with measurements of the model turbine in the laboratory. The two hill diagrams do not correlate. However, for n = 375 when efficiency is plotted against power output, the shape of the two curves are quite similar. The shape of the curve also correlates well with historical data from the Tokke prototype. For n = 375 the average deviation of efficiency between design 1 and the measurements is approximately 2.25%.

It seems like neither the model nor the design 1 would have an efficiency gain if the speed could have been adjusted.

A second simulation design was made, design 2, where $\underline{u}_1$ were changed from 0.72 to 0.80. This was the only parameter changed from design 1. This change leads to a different runner geometry and inlet dimensions. The comparison between design 1 and 2 show that design 1 has higher efficiencies in the normal operating ranges, as well as high load operational areas. Design 2 gives higher efficiencies in part load operational areas.

The results for simulations of design 2, with an adjusted speed of 385 for α =10 and 11 an efficiency gain of approximately 1.2% can be achieved. If n is adjusted to 395 for α = 12 and 13, the efficiencies for design 2 are increased to approximately the same efficiencies as for design 1, at this exact power output. This corresponds to an increase in efficiency, for design 2, of respectively 0.5% and 1% at the mentioned α-values.

The greatest sources of numerical error in the work of this thesis are considered to be simulations with steady-state flow and simulation of only one runner blade in the turbine. Steady state does not capture transient flow phenomena. The greatest sources of design error are caused by neglecting splitter blades as well as only creating a vaneless inlet, runner blade and part of the draft tube. Guide vanes, stay vanes or the spiral casing has not been included in the simulation.

The design and numerical setup must be further improved and validated with experimental results. However, the results in this thesis show are promesing for variable speed operation.

9 Further work

Design 1 of the Tokke prototype made in Khoj yields a hill diagram that is quite different from the hill diagram created with experimental results of the Tokke model in the lab. The efficiencies of design 1 are in general much higher for all operating points and BEP is located far from BEP in the experimental results. More time should be spent on creating a design 1 in closer approximation to the Tokke prototype or model while still keeping a lot of the simplifications intact so the simulation not will cost too much in computational effort.

9.1 Turbine design procedure in Khoj

Khoj is mainly created to design a brand new turbine without any constrains concerning inlet diameter, outlet diameter, head, flow and so on. However, this thesis wants to keep some of these parameters constant so that a new prototype turbine could replace the old prototype turbine at Tokke without having to do too much work and change in the surrounding areas of the runner. Head, volume flow and dimensions (diameter, height, etc.) are parameters which are desired to keep as close to the original prototype as possible. Instead of the standard design approach 'Khoj' uses today, 'Khoj' should be rewritten so that the design process is a better fit for this type of problem.

9.1.1 No correction of synchronous speed

If the turbine will operate at variable speed it is not necessary that 'Khoj' corrects for synchronous rotational speed in the design procedure. A simplified design procedure of the main dimensions if Khoj had not corrected for the synchronous rotational speed is presented. Still designing for BEP keeping head and volume flow constant.

The outlet diameter is still set to 1.8 m and the volume flow is still set to be 31 m^3/s. c_{m2} can then be calculated by equation 7.1.

$$c_{m2} = \frac{4 \cdot Q}{\pi \cdot D_2^2} = 12.18 \qquad [m/s] \tag{7.1}$$

u_2 is set to be 38 m/s which means that β_2 have to be corrected in order to have no swirl at the outlet.

$$\beta_2 = \operatorname{atan}\left(\frac{c_{m2}}{u_2}\right) = 17.77 \qquad [°] \tag{7.2}$$

Now the RPM can be calculated with equation 7.3.

$$n = \frac{u_2 \cdot 60}{\pi \cdot D_2} = 403.2 \qquad [rev/min] \tag{7.3}$$

The speed of rotation will not be corrected for synchronous speed this time. D_1 can now be calculated with equation 7.4. Start by choosing $\underline{u}_1$=0.72 which gives u_1=61.34 m/s from equation 5.4. The effective head is assumed to be 370 m.

$$D_1 = \frac{u_1 \cdot 60}{n \cdot \pi} = 2.9 \quad [m] \tag{7.4}$$

Further, the inlet height can be calculated with equation 7.5.

$$B_1 = \frac{A_1}{\pi \cdot D_1 - z_{blades} \cdot \frac{t_{le}}{sin\beta_1}} = 0.32 \quad [m] \tag{7.5}$$

Where A_1 is calculated with equation 5.8 and β_1 by equation 5.10.

With the new design procedure D_1 will get a different value than if the rotational speed was corrected to synchronous speed. This might lead to a change in the guide vane cascade. The guide vanes usually have a limit to how much they can move within the guide vane area as shown in Figure 40.

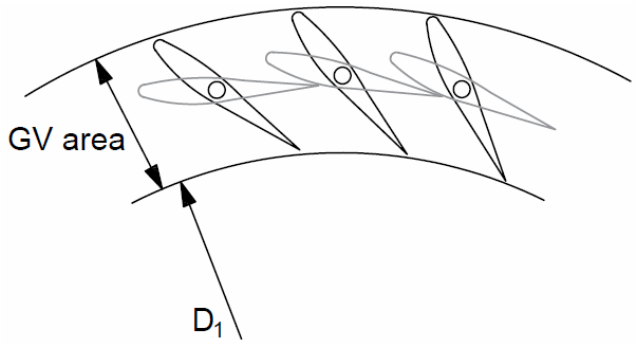

Figure 38 – Guide vane area displaying fully open (black) and fully closed (grey) guide vanes

If the inlet diameter is increased or decreased in too great extent it should be considered to replace the whole guide vane arrangement. For example, if there is a decrease in D_1, the length of the guide vanes must be increased and number of guide vanes should may be decreased. In the opposite case it might be considered to decrease the length and increase the number of guide vanes. Figure 39 and 40 illustrates the changes that may arise from a change in the inlet diameter.

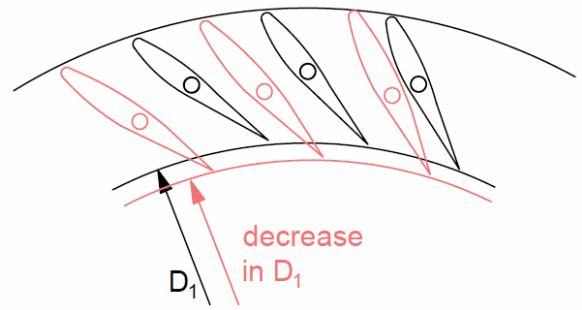

Figure 39 – Example of guide vane design change when there is a decrease in D_1. Fewer and longer guide vanes.

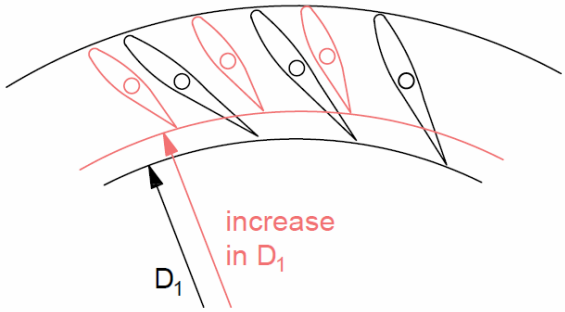

Figure 40 – Example of guide vane design change when there is an increase. More and shorter guide vanes.

With the new design procedure, the inlet diameter will be smaller in all design cases and the inlet height decreases with increasing diameter. It is also noticed that design 1 calculated with the

current design procedure in Khoj have quite similar inlet dimensions as for design 2 with the new design procedure. This is presented in Table 6.

Table 6 – Main dimensions at the Inlet for the different design procedures

	Design procedure in 'Khoj'		**Proposed new design procedure**	
$\underline{u}_1$	D_1 [m]	B_1 [m]	D_1 [m]	B_1 [m]
0.72	3.124	0.296	2.906	0.319
0.75	3.254	0.280	3.027	0.309
0.80	3.471	0.272	3.228	0.294

This can imply that the new design procedure might give more similar inlet dimensions when $\underline{u}_1$ is increased compared to design 1. Further, this could lead to no or small changes in the guide vane cascade.

9.1.2 Keeping the dimensions constant

Another design procedure that might be more convenient for this type of problem would be to have some restrictions concerning the dimensions. In addition to keeping the nominal head and the volume flow constant, the inlet an outlet dimensions, B_1, D_1 and D_2 could also be kept constant to create a design of a turbine that could be fitted into the turbine space at Tokke power plant.

9.2 Investigate more designs

As explained in Chapter 3.4 a normal design of a pump have a $\underline{u}_1$>0.95. It should therefore be investigated if a further increase in $\underline{u}_1$ will show the same trends as the increase from $\underline{u}_1$=0.72 to $\underline{u}_1$=0.8. There is probably several other parameters that should be taken into consideration as well.

9.3 Making draft tube as a separate design

In the draft tube, there is a small cone created in the middle which is not ideal and should be removed in further work. A solution to not creating the cone would be to create the inflow vaneless space and the runner as one geometry and the draft tube as one geometry, mesh them separately and the put the domains together in CFX-pre.

9.4 Further development of mesh

Even though a mesh independence test were conducted, the mesh statistic report shows that the mesh is not optimal either in runner or draft tube domain. The mesh should, therefore, be improved further.

9.5 Investigate impact from excluded parts

During the design of the geometry, guide vanes, stay vanes and the spiral casing is not included. Neither the entire draft tube nor splitter blades are created. The excluding of these components leads to an incomprehensive image of the system. Thus the impact these parts have on the simulation are unknown and should be investigated further.

References

[1] L. Lia (NTNU), T. Jensen (NVE), K. E. Stensby (NVE), G.H. Midttømme(NVE) and A.M. Ruud (Statkraft), *The current status of hydropower development and dam construction in Norway,* Issue 3, p.7(2015). Retrived 21.02.17 from: https://www.ntnu.no/documents/381182060/641036380/Leif+Lia_FINAL.PDF/32bac8f3-b443-493b-a1eb-e22ce572acd9

[2] Gordon E. Moore, *Cramming more components onto integrated circuits* (1965), IEEE Vol. 38 Iss. 8.

[3] H. K. Versteeg and W. Malalasekera (2007), *An Introduction to Computational Fluid Dynamics, The Finite Volume Method*. Harlow, PEARSON Education.

[4] Rainald Löhner (2008), *Applied CFD Techniques, An introduction based on finite Element Methods*. Vol. Second edition. Wiley.

[5] D. Stefan and P. Rudolf, *Proper Orthogonal Decomposition of Pressure fields in a Draft Tube cone of the Francis (Tokke) Turbine Model,* IOPscience, Journal of Physics: Conference Series, Volume 579, conference 1 (2015).

[6] C. Trivedi, M. Cervantes and O.G. Dalhaug, *Experimental and numerical studies of a high-Head Francis Turbine: A review of the Francis-99 Test case.* Energies, 9(2)(2016).

[7] Kristine Gjørsæter, *Hydraulic Design of Francis Turbine Exposed to Sediment Erosion,* Master Thesis, NTNU, Department of Energy and Process Engineering (2011).

[8] Peter Joachim Gogstad, *Hydraulic Design of Francis Turbine Exposed to Sediment Erosion,* Project work, NTNU, Department of Energy and Process Engineering (2011).

[9] C. Farell and J. Gulliver, *Hydromechanics of varable Speed Turbines,* Project report No. 225, University of Minnesota, St. Anthony Falls Hydraulic Laboratory (1983).

[10] S. Muller, M. Deicke and R. W. De Doncker, *Doubly fed induction generator systems,* IEEE Industry applications magazine (2002).

[11] J. I. Perez, J. R. Wilhelmi and L. Maroto, *Adjustable speed operation of a hydropower plant associated to an irrigation reservoir,* Energy Conversion and Management 49 (2008).

[12] A. Borghetti, M. Di Silvestro, G. Naldi, M. Paolone and M. Alberti, *Maximum Efficiency Point Tracking for Adjustable-Speed Small Hydro power plant,* ReaserchGate (2008).

[13] Hermod Brekke, *Pumper og turbiner,* (2003).

[14] Hermod brekke, *Grunnkurs I hydrauliske Strømningsmaskiner,* (2000).

[15] Erik Os Tengs, "*Personal conversations*", 29.01-08.06.2017.

[16] Ole Gunnar Dalhaug, "*Personal conversations"*, 21.03.2017.

[17] Lecture notes in Turbomachinery (TEP4195), *Design of a Francis Runner,* (2016)

[18] Lecture notes in Turbomachinery (TEP4195), *Characteristic values,* (2016)

[19] J. Chawner, *Quality and Control – Two reasons why Structured Grids aren't going away,* The connector, Pointwise (2013).

[20] ANSYS Manual Guide, *ANSYS 16.0 Release Documentation, Theory and Modelling Guide,* p. 2500 (2015).

[21] R. S. R. Gorla and A. A. Khan, *Turbomachinery design and Theory, Chapter 7.6- Free vortex design,* New York: Marcel Dekker, Inc. (2003).

[22] E. Tengs, P-T. S- Stroli and M.A. Holst, *Numerical generation of Hill-Diagrams; Validation on The Francis99 model turbine,* Sent to IJFMS, but not accepted for publishing yet, awaiting approval (2016).

[23] SHARCNET, *2.1.2. CFX Solver,* Realese 17.0. Retrieved 21.05.17 from: https://www.sharcnet.ca/Software/Ansys/17.0/en-us/help/cfx_intr/i1337241.html

[24] F. R. Menter, *Two-Equation Eddy-Viscosity Turbulence Models for Energy Engineering Applications,* AIAA, vol. 32, p.8 (1994).

[25] ANSYS Inc., *ANSYS CFX Solver Theory Guide,* vol. 14.0, p. 89-103 (2011).

[26] G. Alfonsi, *Reynolds- Averaged Navier-Stokes Equations for Turbulence Modeling,* ASME, vol. 62 (2009).

[27] A. L. Holo, *CFD-Analyse av en høytrykks Francis turbin,* Master Thesis, NTNU, Department of Energy and Process Engineering (2011).

[28] M. Cervantes, C. Trivedi, B.K. Gandhi and O.G. Dalhaug, *Experimental and numerical studies for a high head Francis turbine at several operating points,* Journal of fluid engineering, vol. 15 (2013).

[29] A. D. A. Gavrilov, A. Minakov, D. Platonlov and A. Sentyabov, *Steady state operation simulation of the Francis-99 turbine by means of advanced turbulence models*, Journal of physics (2013).

[30] A. Bakker, *Lecture notes ion Computational Fluid Dynamics from Darthmouth College, lecture 7* (2002-2006).

[31] SHARCNET, *21.2.4. Quality Measure,* Release 17.0. Retrived 23.04.2017 from: https://www.sharcnet.ca/Software/Ansys/17.0/enus/help/tgd_usr/tgd_user_report_qualitymeasure.html

Appendix A – Article form CRHT VII'17

This appendix includes the paper written for the International Symposium on current Research in Hydraulic Turbines - VII'17 organized at Kathmandu University as well as some additional information about the Symposium.

The symposium is held at the turbine-testing lab at Kathmandu University. The symposium aims to bring together students, researcher, professionals and experts in the hydro power sector and other renewable fields to share their experience and research insight. This is the seventh time master students from the hydropower lab at NTNU have been present and participated at the symposium. All the master students writes a paper about their project work that is summited a few weeks before arrival. Upon arrival the papers are presented before the symposium. The paper written in connection with this master thesis is attached below. As it was written only two months out in the thesis semester it does not include any notable results, discussion or conclusions.

Proceedings of the International Symposium on Current Research in Hydraulic Turbines

CRHT – VII

April 04, 2016, Turbine Testing Lab, Kathmandu University, Dhulikhel, Nepal

Paper no. _ _ _

Design and Operatioin of a Francis Turbine with Variable Speed Capabilities

Else Høeg Sundfør

Department of Energy and Process Engineering, NTNU, Alfred Getz vei 4, Norway

** Corresponding author (elsehss@yahoo.no)*

Abstract

This paper presents the preliminary work of a master thesis written at the Norwegian University of Science and technology. To balance intermittent energy sources like wind and solar on the grid, flexible hydropower is essential to provide needed power when other renewables cannot deliver enough. To make hydropower more flexible it is suggested to use variable speed operation to keep the hydraulic efficiency as high as possible at all times. This paper deals with the design and simulation procedure for a Francis turbine which will be operated on variable speed. Hill diagrams of different designs are to be made in order to compare new designs with existing designs to see if there is a possible efficiency gain when the turbine is operated on variable speed. The design program 'Khoj' and simulations in ANSYS CFX is presented as well as the procedure for creating the hill diagrams.

Keywords: Francis turbine, Variable speed, CFD, Hill-chart, Hydropower

1. Introduction

1.1 Background

It was recently decided to develop 1000 MW of wind energy in the middle part of Norway. Hydropower is therefore needed to balance intermittent energies like wind and solar on the grid. This means that hydropower have to become more flexible. The most non-flexible limitation for current turbines is fixed speed due to the use of synchronous generators to provide energy to the fixed-frequency electric grid. If the turbines could be operated with variable speed they could be operated as flywheels in case of shut down of intermittent energies and provide the needed power for a short duration until the intermittent energy sources starts producing again. Over-all efficiency could also be improved because the rotational speed could be matched to pressure and flow conditions in at better way.

1.2 Objective

The objective of the full thesis is to optimize a design for a runner intended for variable speed operation for a specific hydropower plant, and preform simulations in order to determine the hill chart for this runner. The power plant chosen is Tokke power plant in Telemark County in Norway. The reason Tokke is chosen is because there is a model version of one of the Tokke turbines in the water laboratory lab at NTNU. The hill chart made with simulations are to be compared with a hill chart of the existing runner in the lab to examine if there is an efficiency gain due to variable speed operation. The efficiency gain will

also be based on historical operation at the real power plant. Since this paper is written in only mid-way in the thesis, many of these objectives have not been fulfilled or even started.

2. Variable speed technology

2.1 Fixed speed topology

In a conventional fixed speed turbine the magnetic field of the stator and the magnetic field of the rotor always rotates with the same speed and the two are coupled . As the grid frequency is constant, the speed of the generator, hence also the turbine is given by:

$$n_{rpm} = \frac{120 \cdot f_{grid}}{p} \tag{1}$$

Where n_{rpm} is the rotational speed, f_{grid} is the frequency of the grid and p is the number of poles in the generator. A turbine that uses fixed speed technology is designed for an optimum value of head and discharge and any variation of these parameters will drive the turbine to an efficiency value lower than the optimum value.

2.2 Variable speed topology

In locations where it is economical and desired to run the turbine at optimum efficiencies, but there are large variations in head or discharge, variable speed operations is required. In a variable speed machine, the stator and the magnetic field of the rotor are decoupled. Either the stator is decoupled from the grid using a frequency converter between the grid and the stator winding, or the rotor field is decoupled by a multiphase rotor winding fed from a frequency converter connected to the rotor[1].

2.3 Benefits with variable speed operation

The hydraulic efficiency depends significantly on both the water discharge, Q and the net head, H_n and is generally represented in a so-called hill chart like in figure 1. If volume flow or head changes there will be a drop in efficiency and other operational problems may also arise. At part load, fixed speed operation with low heads can result in draft tube pressure oscillations and shaft torque fluctuations. In turn fixed speed operation with higher head can cause cavitation[2].

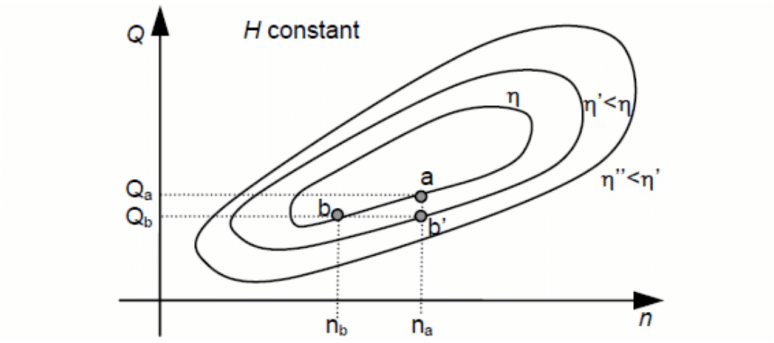

Figure 1 – Example hill chart curve 1 [3]

The idea of variable speed is that if the head or discharge changes, the rotational speed can be adjusted accordingly to maintain high efficiencies. This is demonstrated in figure 1. For fixed speed operation, at a certain head, the efficiency of the turbine will decrease from *a* to *b'* when the discharge decreases from Q_a to Q_b. With variable speed operation the speed can be adjusted from n_a to n_b to obtain an efficiency in

point *b* which is equivalent to the efficiency in point *a*. Consequently a variable speed turbine permits maximum efficiency tracking for a given power demand. This kind of operation is only possible if the hill chart looks similar to the one in figure 1. If the hill chart curve is more symmetrical like in figure 2, adjusting the speed either direction will not affect the efficiency. The goal is therefore to try to make a turbine design, which ultimately can yield a hill chart curve that looks similar to the one in figure 1.

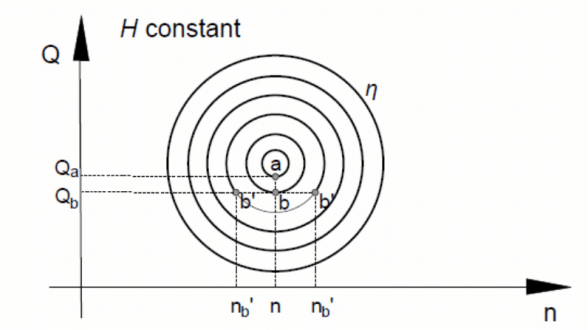

Figure 2 – Example of hill chart curve 2

3. Tokke Power plant

Tokke power plant is located in Telemark County and is owned by Statkraft. Four Francis turbines with a total output of 430 MW (107.5 each) was installed in 1960 and the turbines will probably need replacement in near future. The turbines run at constant speed of 375 rpm with a waterfall of 377 m and a flow rate of 31 m^3/s at BEP. The water laboratory at NTNU has a scaled prototype of one of the turbines at Tokke. The prototype is used to obtain test records of operations and provide hill charts of the turbine. These hill charts will be compared with the simulated designs. In addition to this Statkraft have provided a historical operation of one of the real turbines at Tokke for a period of 23 hours displayed in figure 3. The efficiency of the historical operation will be compared to simulation values for the same power output.

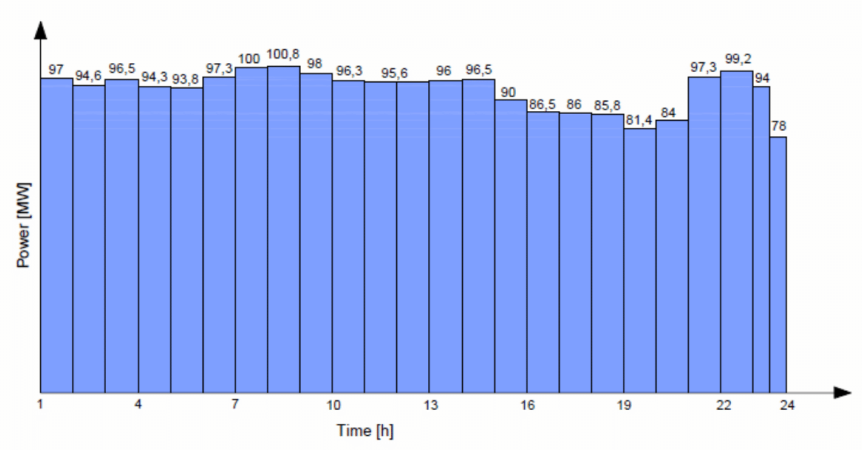

Figure 3 – 23 hour operation run at Tokke

4. ‘Khoj’ – Turbine design software

In 2011, during her master thesis Kristine Gjøsæter started developing the in-house design software ‘Khoj’ which has been further modified until this day[4, 5]. ‘Khoj’ is a Francis design software programmed in Matlab with a graphical user interface and the background information for the design software can be found in her master thesis – Hydraulic Design of Francis Turbine Exposed to Sediment Erosion[4]. There are 17 activated parameters within the blade design stage, displayed in Table 1, which can be altered with and adjusted to optimize a specific design. Within the constraints of the input parameters the profile of one blade of the runner is created and exported back to ANSYS workbench where 3D coordinates of the blade component are obtained. The coordinates for the Hub, shroud, draft tube and inlet are also created. Output parameters calculated by ‘Khoj’ is displayed in table 2.

Table 1 – Input parameters for blade design

Parameter name	**Description**	**Unit**
Q	Volume flow	[m^3/s]
H	Head	[m]
U2	Outlet peripheral velocity	[m/s]
beta2	Outlet blade angle	[°]
acc	Acceleration from inlet to outlet	[-]
t_te	Thickness trailing edge	[mm]
t_le	Thickness leading edge	[mm]
Z_b	Number of runner blades	[-]
Z_gv	Number of guide vanes	[-]
Z_sv	Number of stay vanes	[-]
u_1red	Inlet reduced peripheral velocity	[-]
b_ellipse	The shroud has an elliptic form, b says something about the size	[?]
ns	Numerical parameter, recommended >20 [6]	[-]
div	Numerical parameter, recommended >20 [6]	[-]
a_ss	Ellipse form leading edge suction side	[mm]
a_ps	Ellipse form leading edge pressure side	[mm]
GV	Guide vanes, 1= Yes, 0= No.	[-]

Table 2 – Output parameters

Parameter name	**Description**	**Unit**
D2	Outlet diameter	[m]
Blades	Number of runner blades	[-]
Alpha	Guide vane angle	[°]
RPM	Revolutions per minute	[-]

3.1 Design restrictions

As described in the objective of this paper, the design of the runner have to be optimized for variable speed operation for a specific hydropower plant. This limits the design to some degree since head, flowrate and diameter have to be approximately the same as before. Changes in head are possible to vary to some extend without extra cost, but flowrate through the channels will be quite expensive to alter. The diameter can be altered with to some degree, but this will affect the guide vanes in length and number.

5. Meshing in TurboGrid

A good mesh is essential to achieve reliable results. According to ANSYS TurboGrid automatically produces high quality hexahedral meshes needed for blade passages in rotating machinery. The mesh created in TurboGrid is a structured mesh consisting hexahedra cells. Structured meshes give the quality

and control to generate precisely the mesh you need and are widely acknowledged to be superior to unstructured meshes[7]. According to Chawner (2013), hexahedron cell fills the same volume as tetrahedron cells with fewer amounts of cells thereby lowering both CPU time and memory. In addition high quality cells are easily generated on a hex grid with high aspect ratio and the CFD solver converge better and produce more accurate results when the mesh is aligned with the predominant flow direction, which is the case for structured meshes as the mesh lines follow the curve of the geometry.

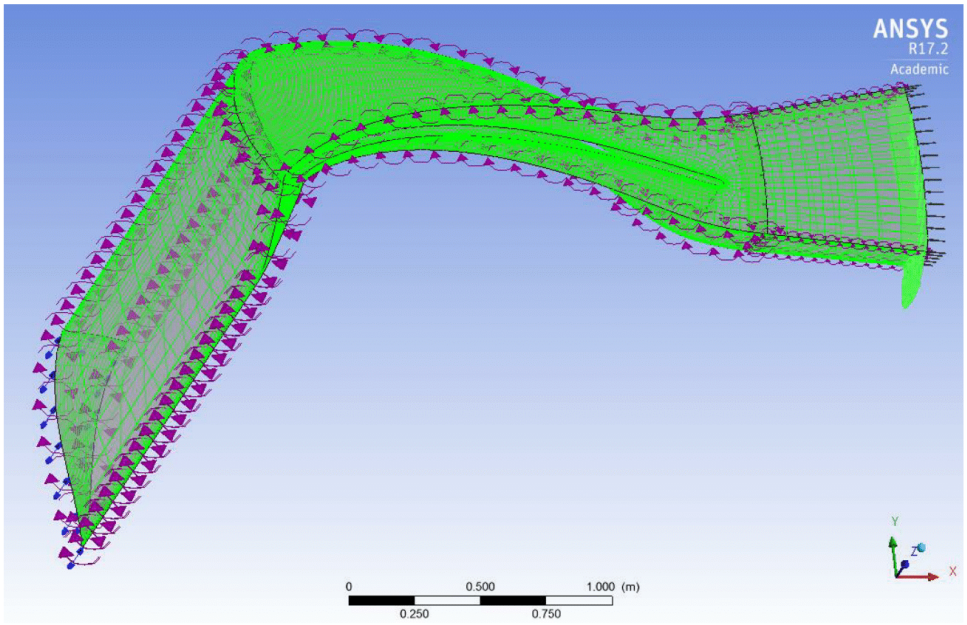

Figure 4 – TurboGrid meshing of one section including inlet, runner and draft tube

A thorough mesh convergence test will be conducted to ensure that the results of the analysis are not affected by changing the size of the mesh. Number of nodes will be plotted against important global output values like head, flow and hydraulic efficiency to establish mesh convergence. The simulations preformed so far have been inconclusive due to some mesh setup mistakes in TurboGrid. The mesh convergence test will be done applying a coarse mesh, a medium mesh and fine mesh. If needed even finer meshes will be made if it does not affect the computational time to significant degree. In figure 5, 6 and 7 three different mesh sizes over a single runner blade is shown.

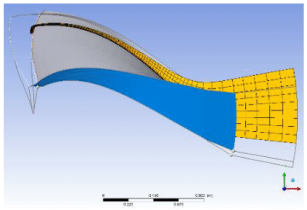

Figure 5 – Coarse grid size with approximately 20.000 nodes

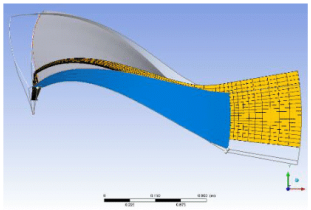

Figure 6 – Medium grid size with approximately 100.000 nodes

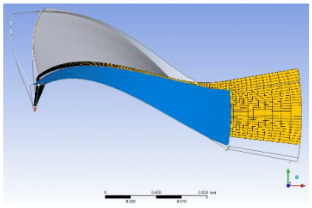

Figure 7 – Fine size grid with approximately 250.000 nodes

6. ANSYS CFX – Simulation solver

The simulations are done in steady state due to lack of computational time as well as it easier to post process and analyze even though transient is preferable for rotating machinery. The applied turbulence model is shear stress transport due to its benefits of combining k-ω and k-ε. It utilizes the original k-ω model of Wilcox in the inner region of the boundary layer and switches to the standard k-ε model in the outer region and in free shear flows[8].

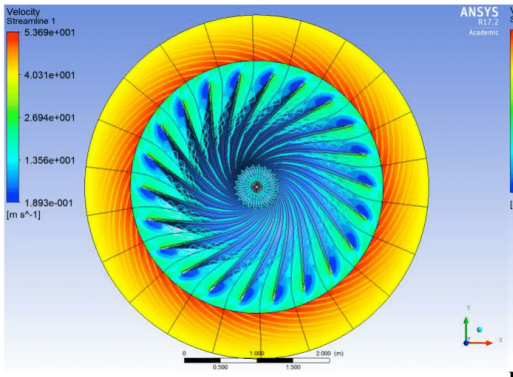

Figure 8 – Result of arbitrary simulation displaying pressure distribution and velocity streamlines, viewed from above in X-Y coordinate

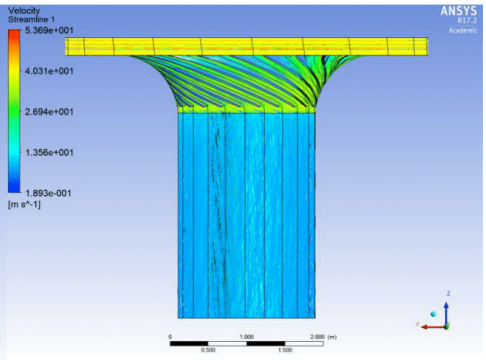

Figure 9 – Result of arbitrary simulation displaying pressure distribution and velocity streamlines, viewed from the side in X-Z coordinate

The process is set to be isothermal with a fluid temperature of between 5-10°C. Buoyancy turbulence will be considered switched from 'none' to 'production and dissipation'. This is due to some internet forums regarding CFD claiming that enabling this function will yield greater resolution on the interface between layers that might form and that it is more accurate. It is also pointed out that this might demand more computational time.

7. Creation of hill diagram

To create a hill diagram in the lab one keeps the guide vane opening constant while varying the speed. The flow, head and torque is measured and the efficiency is calculated as the ratio between supplied energy and delivered energy to the turbine shaft. This is repeated for a number of different guide vane openings. As a rule of thumb the speed of rotation is regulated in the range of ±20 % from BEP and guide vane opening, alpha, is regulated range of ±40% from BEP when doing measurements.

Essentially the exact same procedure is used when creating a hill diagram in ANSYS and Matlab. A new workbench called Hill was created in ANSYS including a CFX simulation where the design and mesh is imported. The CFX solution setup was then connected to a block called response surface where it is possible to run the turbine at different RPM and alpha values. RPM and alpha are chosen as input parameters and efficiency, head and flow are chosen as output parameters. Alpha is chosen to be between 6-14 with 1-degree interval and RPM to be in the range between 300-450 with an interval of 15. Figure 10 is a display of a design run at 10 degrees at 11 different speeds of rotation. The procedure is repeated for nine different values of alpha.

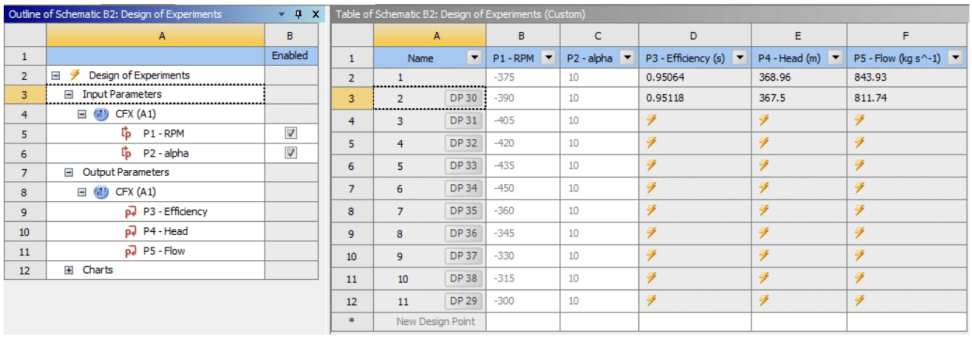

Outline of Schematic B2: Design of Experiments

	A	B
1		Enabled
2	Design of Experiments	
3	Input Parameters	
4	CFX (A1)	
5	P1 - RPM	☑
6	P2 - alpha	☑
7	Output Parameters	
8	CFX (A1)	
9	P3 - Efficiency	
10	P4 - Head	
11	P5 - Flow	
12	Charts	

Table of Schematic B2: Design of Experiments (Custom)

	A	B	C	D	E	F
1	Name	P1 - RPM	P2 - alpha	P3 - Efficiency (s)	P4 - Head (m)	P5 - Flow (kg s^-1)
2	1	-375	10	0.95064	368.96	843.93
3	2 DP 30	-390	10	0.95118	367.5	811.74
4	3 DP 31	-405	10			
5	4 DP 32	-420	10			
6	5 DP 33	-435	10			
7	6 DP 34	-450	10			
8	7 DP 35	-360	10			
9	8 DP 36	-345	10			
10	9 DP 37	-330	10			
11	10 DP 38	-315	10			
12	11 DP 29	-300	10			
*	New Design Point					

Figure 10 - Hill workbench setup, design of experiments. Displays a specific design where alpha is kept constant at 10 and RPM is varied from 300 to 450 with an interval of 15

The hill chart is expressed in unit values n_{11} and Q_{11} where Q is flow rate, D is diameter, H is head and n is rotational speed. A Matlab script that is not yet been written will sketch the hill charts for the different designs.

$$Q_{11} = \frac{Q}{D^2 \cdot \sqrt{H}} \tag{2}$$

$$n_{11} = \frac{n \cdot D}{\sqrt{H}} \tag{3}$$

8. Results and discussion

For comparative reasons the design of Tokke power plant will be recreated in 'Khoj' in as close approximation as possible to the real power plant. A hill diagram from the Tokke model in the lab will be compared to a hill diagram with the simulation of the real plant. This is done to get an idea of how accurate the simulation is. Then different designs will be tried out to determine a possible efficiency gain. If there is enough time a Matlab script that automatically can compare the hill diagrams and efficiency gain at several different operational points will be created.

9. Conclusion

At the time of writing this paper no design suggestion can be made since most of the time so far have been used to get familiar with ANSYS CFX and 'Khoj' as well as deciding the mesh setup.

Acknowledgement

I would like to acknowledge and extend my gratitude to my supervisor Pål Tore Selbu Storli and co-supervisor Ole Gunnar Dahlhaug for their help through both my project thesis and master's thesis. I would also like to thank the industrial PhD candidate Erik Os Tengs that constantly helps me with ANSYS CFX and for his ideas and insight.

References

[1] M. D. R. W. D. D. S. Muller, "Doubly fed induction generator systems," *Industry applications magazine,* 2002.

[2] J. R. W. a. L. M. J.I. Perez, "Adjustable speed operation of a hydropower plant associated to an irrigation reservoir," 2008.

[3] M. D. S. A. Borghetti, G. Naldi, M. Paolone and M. Alberti, "Maximum Efficiency Point Tracking for Adjustable-Spedd Small Hydro Power Plant," 2008.

[4] K. Gjøsæter, "Hydraulic Design of Francis Turbine Exposed to Sediment Erosion," 2011.

[5] P. J. Gogstad, "Hydraulic design of Francis turbine exposed to sediment erosion," 2011.

[6] E. O. Tengs, "- Personal conversations," 26.02.2017.

[7] J. Chawner, "Quality and Control - Two Reasons Why Structured Grids Aren't Going Away," *The Connector, Pointwise,* 2013.

[8] F. R. Menter, "Two-Eqation Eddy-Viscosity Turbulence Models for Engineering Applications," *AIAA,* vol. 32, August, 1994.

Appendix B - Matlab code for creating hill diagram

```
%HillDiagrammet
close all
clear all
clc
load('Verdier.mat')

%Converts the vectors to matrices, only needed for head, etha, ned and Qed

Head = reshape(Head,[15,9]);
eta = reshape(eta,[15,9]);
ned = reshape(ned,[15,9]);
Qed = reshape(Qed,[15,9]);

%Plotting of hill diagram

%Defining the look of the alpha values
LINESPEC=cellstr(['-k+'; '-ko'; '-k*'; '-k.'; '-kx'; '-kh'; '-kd';...
    '-k^'; '-kv'; '-k<'; '-k>'; '-kp'; '-kh';]);
fontSizeLabel=11; fontSizeAxes=11; fontweight='bold';

 %Best point values
[M,I] = max(eta(:));
[I_rad, I_kol] = ind2sub(size(eta),I);

 NedStar = ned(I_rad,I_kol);
 etaStar = eta(I_rad,I_kol);
 QedStar = Qed(I_rad,I_kol);

%Plot HillDiagram

%FIrstly Eta is plotted against ned
figure(1)
clf; %clear this figure
textPosition=[0.232 91.7];
axes('fontSize', fontSizeAxes, 'fontWeight', fontweight)
hold on;

for m = 9:-1:1
plot(ned(:,m),eta(:,m)*100, LINESPEC{m})
end
hold on

text(textPosition(1),textPosition(2)-0.7,['\eta*=', num2str(etaStar)],...
    'fontSize' , fontSizeLabel, 'fontWeight', fontweight);
text(textPosition(1),textPosition(2),['Ned*=', num2str(NedStar)],...
    'fontSize' , fontSizeLabel, 'fontWeight', fontweight);
xlabel('Ned [2]', 'fontSize' , fontSizeLabel ) ; ...
    ylabel('Efficiency  \eta [%]', 'fontSize' , fontSizeLabel);
legend( '\alpha=14', '\alpha=13' , '\alpha=12', '\alpha=11', ...
    '\alpha=10', '\alpha=9' , '\alpha=8', '\alpha=7','\alpha=6', ...
    'Location', 'NorthEast'); legend('boxoff');
```

```
axis([0.15 0.24 68 100 ])

%Qed plotted against ned
figure(2)
clf;
textPosition = [0.232 0.18];
axes('fontSize', fontSizeAxes, 'fontWeight', fontweight)
hold on;

for n = 9:-1:1
plot(ned(:,n),Qed(:,n), LINESPEC{n})
end

grid on;
text(textPosition(1),textPosition(2)-0.04, ['Qed*=',num2str(QedStar)],...
    'fontSize',fontSizeLabel, 'fontWeight', fontweight);
text(textPosition(1),textPosition(2)-0.05,['Ned*=', num2str(NedStar)],...
    'fontSize' , fontSizeLabel, 'fontWeight', fontweight);
xlabel('Ned [2]', 'fontSize' , fontSizeLabel ) ; ylabel(' Qed [2]', ...
    'fontSize' , fontSizeLabel);
legend('\alpha=14', '\alpha=13' , '\alpha=12', '\alpha=11', '\alpha=10',...
    '\alpha=9' , '\alpha=8', '\alpha=7' ,'\alpha=6', 'Location',...
    'NorthEast');
legend('boxoff');
axis([0.14 0.24 0.04 0.23 ])


%Plotting BEP
plot(NedStar, QedStar,'or')

    NN = 81;
    Xstart = 0.15;
    Xslutt = 0.22;
    x = linspace(Xstart,Xslutt,NN);

    n = zeros(NN,9);
    q =n;
    e=n;


    [a,b]=size(ned);
    for i=1:1:b
    q(:,i)=interp1(ned(:,i), Qed(:,i), x,'PCHIP','extrap');
        %Ned against Qed (with extrapolation)
    e(:,i)=interp1(ned(:,i), eta(:,i), x,'PCHIP','extrap');
    %Ned against eta (with extrapolation)

    end

    N=zeros(NN,NN); Q=N; E=Q;

for i=1:NN
    N(:,i)=x;
    Q(i,:)=linspace(0.22, 0.06, NN); %The area that Qed is plotted for
```

```
    E(i,:)=interp1(q(i,:), e(i,:),Q(i,:),'PCHIP','extrap');
end

% Creating hill diagram lines
figure(2);
grid on
v=[97.2 97.1 97 96.75 96.5 96.2 96 95.5 95 94.5 94 93 91 90 88]/100;
% The values for v is altered for each hill diagram to make suitable
% hill diagram lines
[C,h]=contour(N, Q, E,v);
set(h,'LineStyle','-','LineColor','k')
clabel(C, h,'fontSize' , fontSizeLabel, 'fontWeight', fontweight)
```

Published with MATLAB® R2015a

Appendix C – Input and output parameters for turbine design

This appendix presents the design input and output parameters for the design similar to Tokke that is used in the grid convergence test and simulated in ANSYS CFX. Three different design input and output parameters are presented.

Table 7 – Input parameters for initial blade design, $\underline{u}_1$=0.72

Parameter name	Description	Initial design inputs	Unit
Q	Volume flow	31	[m^3/s]
H	Nominal head	377	[m]
u_2	Outlet peripheral velocity	38	[m/s]
β_2	Outlet blade angle	19	[°]
acc	Acceleration from inlet to outlet	1.1	[2]
t_te	Thickness trailing edge	10	[6]
t_le	Thickness leading edge	20	[6]
z_b	Number of runner blades	17	[2]
$\underline{u}_1$	Inlet reduced peripheral velocity	0.72	[2]
b_ellipse	The shroud has an elliptic form, b says something about the size	0.69	[?]
ns	Numerical parameter, recommended >20 [7]	40	[2]
div	Numerical parameter, recommended >20 [7]	40	[2]
a_ss	Ellipse form leading edge suction side	30	[6]
a_ps	Ellipse form leading edge pressure side	10	[6]
GV	Guide vanes, 1= Yes, 0= No.	0	[2]

Table 8 – Output parameters from blade design

Parameter name	Description	Initial output parameters	Unit
D_2	Outlet diameter	1.8006	[m]
Blades	Number of runner blades	17	[2]
Alpha	Guide vane angle	8.0912	[°]
RPM	Revolutions per minute	375	[2]

Table 9 - Input parameters for initial blade design, $\underline{u}_1$=0.80

Parameter name	Description	Initial design inputs	Unit
Q	Volume flow	31	[m^3/s]
H	Nominal head	377	[m]
u_2	Outlet peripheral velocity	38	[m/s]
β_2	Outlet blade angle	19	[°]
acc	Acceleration from inlet to outlet	1.1	[2]
t_te	Thickness trailing edge	10	[6]
t_le	Thickness leading edge	20	[6]
z_b	Number of runner blades	17	[2]
$\underline{u}_1$	Inlet reduced peripheral velocity	0.80	[2]
b_ellipse	The shroud has an elliptic form, b says something about the size	0.69	[?]
ns	Numerical parameter, recommended >20 [7]	40	[2]
div	Numerical parameter, recommended >20 [7]	40	[2]
a_ss	Ellipse form leading edge suction side	30	[6]
a_ps	Ellipse form leading edge pressure side	10	[6]
GV	Guide vanes, 1= Yes, 0= No.	0	[2]

Table 10 – Output parameters from blade design

Parameter name	Description	Initial output parameters	Unit
D_2	Outlet diameter	1.8006	[m]
Blades	Number of runner blades	17	[2]
Alpha	Guide vane angle	8.9763	[°]
RPM	Revolutions per minute	375	[2]

Appendix D – Mesh Quality Theory

Mesh Orthogonality

Maximum and minimum face angle is considered a measure of skewness, which is one of the primary quality measures for a mesh. Skewness determines how close to ideal a face of a cell is.

Maximum face angle is the greatest face angle for all faces that touch the node. For each face, the angle between the two edges of the face that touch the node is calculated (31). The largest angle from all the faces is returned. Minimum face angle, on the other hand, is the smallest angle for all faces that touches the node.

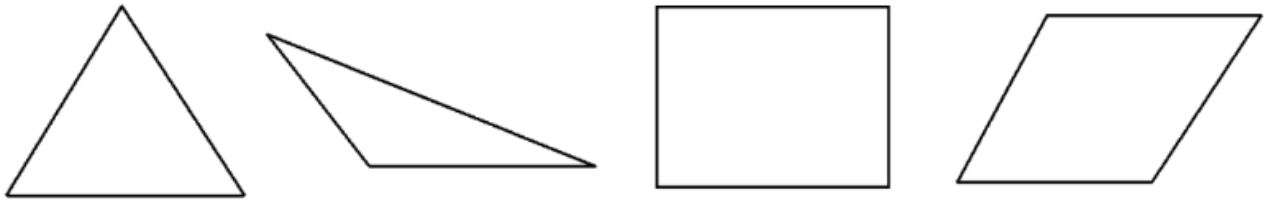

Ideal Triangle | Skewed Triangle | Ideal Quad | Skewed Quad

SHARCNET lists a range of skewness values and the corresponding cell quality (30,31). According to the definition, a value of zero indicates the best quality and a value of one indicates a completely degenerate cell. A skewness value above one are considered invalid, and according to Bakker (30) for hexahedral cells the skewness should not exceed 0.85.

Value of Skewness	0 – 0.25	0.25 – 0.5	0.5 – 0.8	0.8 – 0.95	0.95 – 0.99	0.99 – 1.0
Cell Quality	Excellent	Good	Acceptable	Poor	Silver	Degenerate

Mesh expansion

Mesh expansion relates to how much adjacent elements change in area or volume compared to each other. In ANSYS element volume ratio represents mesh expansion and an acceptable range of this measure is said to be below 20 (31).

Element volume ratio is the ratio between the maximum volume of an element that touches a node and the minimum volume of an element that touches a node. The returned value can be used as a measure of the local expansion factor.

Aspect ratio

The aspect ratio of the mesh relates to what degree the mesh elements are stretched. It is the ratio of the longest to the shortest side in a cell. Ideally, it should be equal to one to ensure the best results and local variations should be kept to a minimum. According to several sources, variations in adjacent cells should not exceed 20% (30). Having a large aspect ratio can result in an interpolation error of unacceptable magnitude and will lead to round-off errors and difficulties

with converging the equations. The acceptable range for both aspect ratio and edge length ratio is according to SHARCNET both below 100. The edge length ratio can be considered a measure of aspect ratio.

Mesh independence

A mesh convergence test is usually conducted to ensure that the results of the analysis are not affected by changing the size of the mesh. Number of nodes or elements are plotted against important parameters.

Appendix E – Solver Theory

The set of equations solved by ANSYS CFX is the unsteady Navier-Stokes equations in their conservative form. The instantaneous equation of mass, momentum and energy conservation in a stationary frame can be written as follows(25):

The continuity equation:

$$\frac{\partial \rho}{\partial t} + \nabla \cdot (\rho U) = 0 \tag{E.1}$$

Where U is the velocity vector $U_{x,y,z}$.

The momentum equations:

$$\frac{\partial (\rho U)}{\partial t} + \nabla \cdot (\rho U \otimes U) = -\nabla p + \nabla \tau + S_M \tag{E.2}$$

Where S_M is a source term and the stress tensor, τ, is related to the strain rate by:

$$\tau = \mu(\nabla U + (\nabla U)^T - \tfrac{2}{3}\delta \nabla \cdot U) \tag{E.3}$$

The total energy equation:

$$\frac{\partial (\rho h_{tot})}{\partial t} - \frac{\partial p}{\partial t} + \nabla(\rho U h_{tot}) = \nabla(\lambda \nabla T) + \nabla(U \cdot \tau) + U \cdot S_M + S_E \tag{E.4}$$

Where h_{tot} is the total enthalpy, related to the static enthalpy $h(T, p)$ by:

$$h_{tot} = h + \frac{1}{2}U^2 \tag{E.5}$$

The term $\nabla(U \cdot \tau)$ represents the work due to viscous stresses and is called the viscous term. Internal heating due to viscosity in the fluid, and is negligible in most flows. The term $U \cdot S_M$ represents the work due to external momentum sources and is currently neglected.

The Navier-Stokes equations describe both laminar and turbulent flow without the need for additional information. Turbulence occurs when inertia forces in the fluid become significantly larger compared to viscous forces. Turbulent flows at realistic Reynolds numbers would involve length scales much smaller than the smallest finite volume mesh. The direct numerical simulation (DNS) of these types of flows would require computing power which is many orders of magnitude higher than available in the foreseeable future. Turbulence models have been specifically designed to account for the effects of turbulence without the use of a highly fine mesh and direct numerical simulation. In general, turbulence models seek to modify the original unsteady Navier-Stokes equations by the introduction of averaged and fluctuation quantities to produce the Reynolds Averaged Navier-Stokes (RANS) equations. These equations represent the mean flow quantities only while modeling turbulence effects without the need for the resolution of the turbulent fluctuations. This averaging procedure introduced additional unknown terms

containing products of the fluctuating quantities which act like additional stresses in the fluid. These terms, called 'turbulent' or 'Reynolds' stresses, are difficult to determine directly and so becomes further unknowns. The Reynolds turbulent stresses need to be modeled by additional equations of known quantities to achieve closure. Closure implies that there are sufficient enough equations for all the unknown, including the Reynolds stress tensor resulting from the averaging procedure. The equations used to close the system defines the type of turbulence model. CFX can broadly be divided into two classes of turbulence models: Eddy viscosity models and Reynolds average stress models. SST turbulence model belongs under Eddy viscosity model and is a two-equation turbulence model.

SST turbulence model

Two- equation turbulence models are very widely used as they offer a good compromise between numerical effort and computational accuracy. Two equation models are more sophisticated than zero equation models. Both the velocity and the length scale are solved using separate transport equations (hence the term 'two equation'). In two equation models, the turbulence velocity scale is computed from the turbulent kinetic energy. The turbulent length scale is often estimated from two properties of the turbulence field. These two often include the turbulent kinetic energy and its dissipation rate. The dissipation rate of the turbulent kinetic energy is provided from the solution of its transport equation.

The proper transport behavior can be obtained by a limiter to the formulation of the eddy-viscosity given in the following equations.

$$v_t = \frac{a_1 k}{\max(a_1 \omega, SF_2)} \tag{E.6}$$

Where

$$v_t = \mu_t / \rho \tag{E.7}$$

and μ_t is the turbulence viscosity.

F_2 is a blending function which restricts the limiter to the wall boundary layer, as the underlying assumptions are not correct for free shear flow. S is an invariant measure of the strain rate. The blending functions are critical to the success of the method. Their formulation is based on the distance to the nearest surface on the flow variables.

$$F_2 = \tanh(arg_2^2) \tag{E.8}$$

With:

$$arg_2 = \max\left(\frac{2\sqrt{k}}{\beta' \omega y}, \frac{500\nu}{y^2 \omega}\right) \tag{E.9}$$

Where y is the distance to the nearest wall and v is the kinematic viscosity. The following choice of freestream values is, according to Menter, recommended:

$$\omega_\infty = (1 \to 10)\frac{U_\infty}{L} \qquad \nu_{t\infty} = 10^{-(2\to5)}\nu_\infty \qquad k_\infty = \nu_{t\infty}\omega_\infty$$

L is the approximate length of the computational domain. Further the boundary condition for ω at a solid surface is:

$$\omega = 10\frac{6\nu}{\beta_1(\Delta y_1)^2} \quad at \quad y = 0 \tag{E.10}$$

Where $\Delta y_1$is the distance to the next point away from the wall and the constants are defined as follows.

β'	= 0.09	β_1	= 0.0705
a_1	= 0.31	κ	= 0.41
σ_{k1}	= 0.85	$\sigma_{\omega1}$	= 0.5
γ_1	= β_1/β'-$\sigma_{\omega1}\kappa^2/\sqrt{\beta'}$		

The values of k and ε come directly from the differential transport equations for the turbulence kinetic energy and turbulence dissipation rate.

Appendix F – Uncertainty analysis of simulations and mesh statistics

Uncertainty analysis and mesh statistics for u_1=0.72

To get a sense of the uncertainty in the global output values one point was observed in the solver monitor. This point chosen to monitor had an alpha value of 9 and a RPM of 375. Figure 31-34 displays the monitor overview for the flow, head, efficiency and for mass and momentum respectively for approximately 300 iterations. This is done to make sure that the global parameters converge to a degree that is "sufficient enough" to trust the solver run. Min and max shows the minimum and maximum value of flow, head and efficiency for the last 100 iterations. These values yield the uncertainty range for the results from this design.

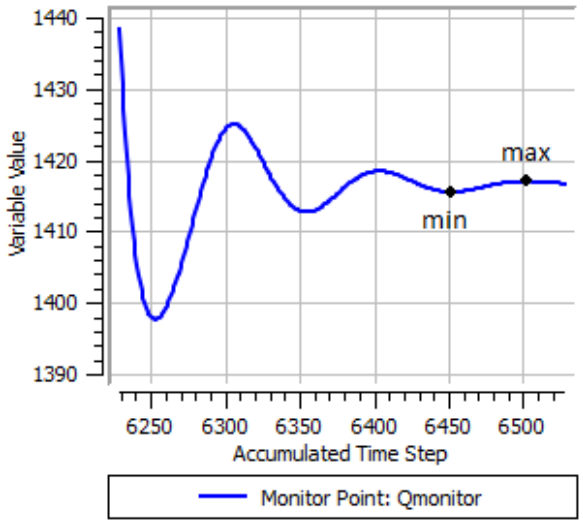

Figure 41 - Monitor overview of the flow for one run (approximately 300 iterations).

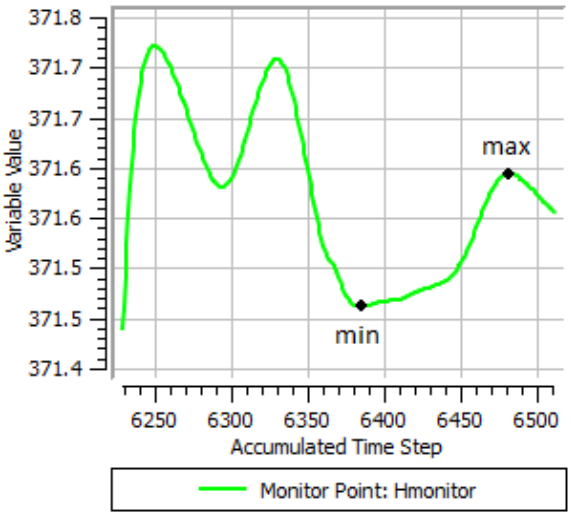

Figure 42 - Monitor overview of the flow for one run (approximately 300 iterations).

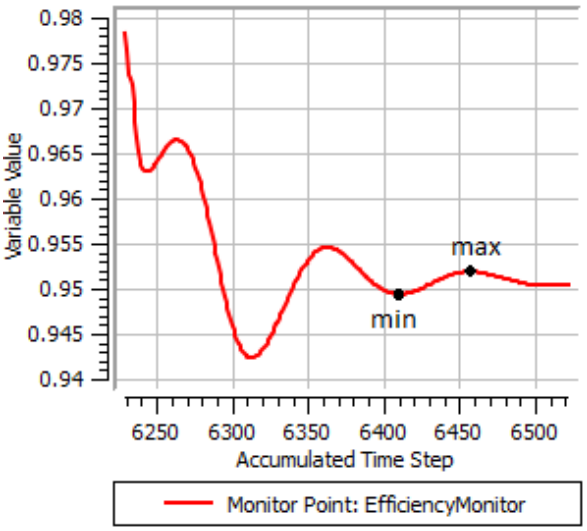

Figure 43 - Monitor overview of the flow for one run (approximately 300 iterations).

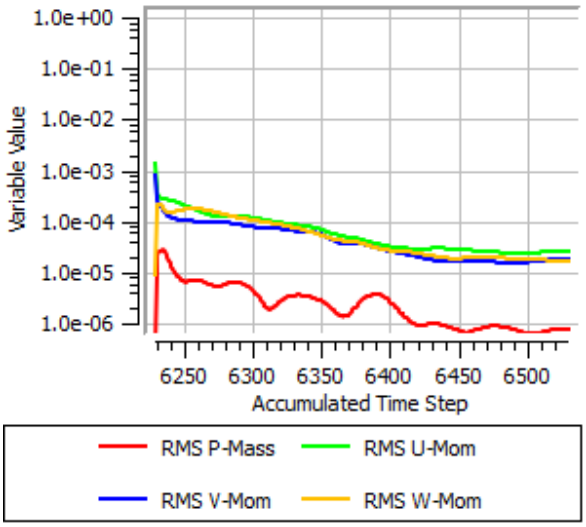

Figure 44 - Residual monitor overview of mass and momentum for one run (approximately 300 iterations)

Table 6 shows a summary of the uncertainty values. The minimum or maximum value furthest away from the value when the solution converged were chosen as the uncertainty value. The flow has a uncertainty of 0.12 %, head has an uncertainty of 0.02 % and the efficiency an uncertainty of 0.13%.

Table 11 - Uncertainty calculations of flow, head and efficiency for a single point where alpha=9 and RPM=385

	Minimum of last 100 iterations	The value where the iterations stopped	Maximum of the last 100 iterations	Uncertainty	%
Flow [m^3/s] (all 17 blades)	24.06	24.08	24.114	0.034*	0.12
Head [m]	371.46	371.55	371.59	0.09*	0.02
Efficiency [2]	0.950	0.9506	0.9518	0.09*	0.13

*The min. or max. value furthest from the value when the iterations stopped was chosen as the uncertainty value

Mesh statistics for this mesh is displayed in Table 7. The mash statistics are based on the mesh limits chosen in the TurboGrid mesh setup discussed in Chapter 6.2.2. Orthogonal angle, expansion factor and aspect ratio are considered as either good, acceptable or poor. Good is annotated with 'OK', acceptable with 'ok' and poor with '!'. The minimum or maximum value is presented for the different measures including the percentage distribution of good, acceptable or poor within the domain.

Table 12 - Mesh statistics, $\underline{u}_1$=0.72

Domain name	Orthogonal Angle Minimum [deg]	Expansion Factor Maximum	Aspect Ratio Maximum
Draft tube	49.5 (1%, 99 %OK)	3 (100 %OK)	1998 (3 %!, 16 %ok, 81%OK)
Inflow	66.7 (100 %OK)	2 (100 %OK)	231 (9 %ok, 91 %OK)
Runner	36.4 (17 %ok, 83 % OK)	5 (100 %OK)	276 (<1 %ok, 100 %OK)
Global	36.4 (15 %ok, 85 % OK)	5 (100 %OK)	1998 (<1 %!, 2 %ok, 98 %OK)

Uncertainty analysis and mesh statistics for $\underline{u}_1$=0.80

To be able to say something about the uncertainty of the numerical results where $\underline{u}_1$ is 0.8, the flow, head, efficiency and residual targets for mass and momentum are observed for one point in time step monitors, same as for $\underline{u}_1$=0.72. The run that was chosen to observe had an alpha value of 11 and RPM of 375. Even though the uncertainty test is only done for one design point, most design points converged with similar acceptable deviation. Figure 26-28 displays the overview of flow, head and efficiency respectively. Figure 30 gives an overview of the residuals for mass and momentum.

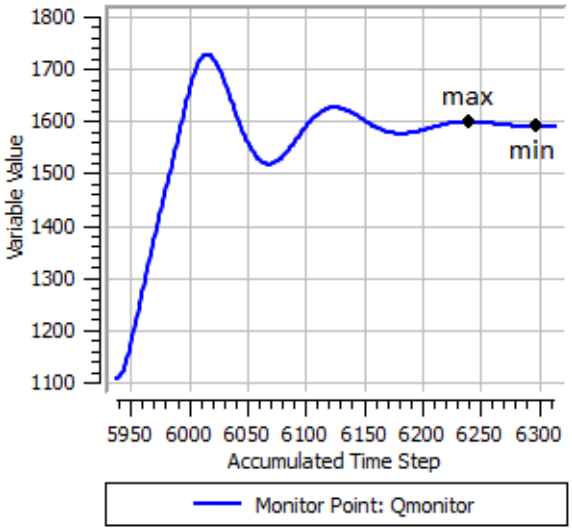

Figure 45 – Monitor overview of the flow for one run (approximately 400 iterations).

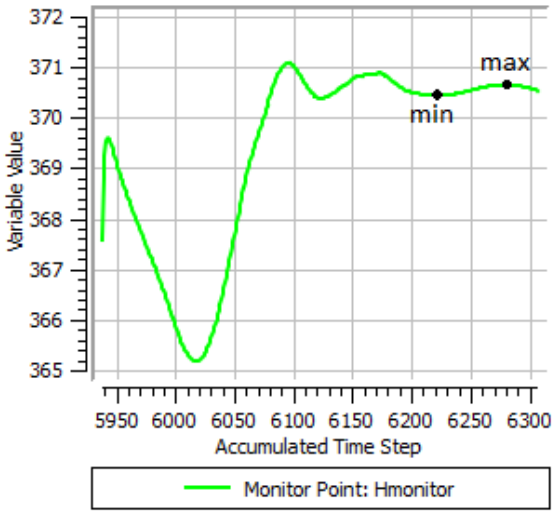

Figure 46 - Monitor overview of the head for one run (approximately 400 iterations).

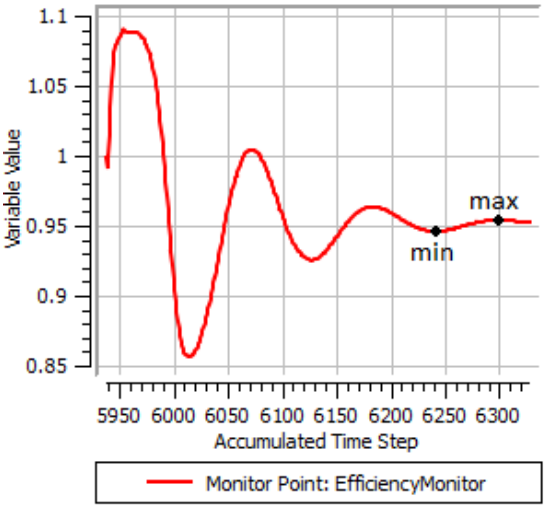

Figure 47 - Monitor overview of the efficiency for one run (approximately 400 iterations).

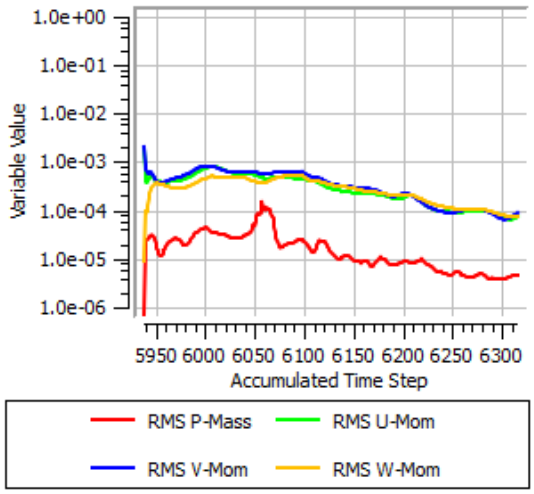

Figure 48 – Residual monitor overview of mass and momentum for one run (approximately 400 iterations)

Table 8 shows a summary of the uncertainty values. The flow has a uncertainty of 0.44 %, head has an uncertainty of 0.06 % and the efficiency an uncertainty of 0.58%. The uncertainty values for $\underline{u}_1$=0.8 is 3-4 times higher than the uncertainty values for $\underline{u}_1$=0.72.

Table 13 – Uncertainty calculations of flow, head and efficiency for a single point where alpha=11 and RPM=375

	Minimum of last 100 iterations	The value where the iterations stopped	Maximum of the last 100 iterations	Uncertainty	%
Flow [m^3/s] (all 17 blades)	27.01	27.064	27.183	0.179*	0.44
Head [m]	370.39	370.43	370.66	0.23*	0.06
Efficiency [2]	0.946	0.95153	0.95379	0.00553*	0.58

*The min. or max. value furthest from the value when the iterations stopped was chosen as the uncertainty value

Further on Table 9 gives and overview of the mesh statistics for this design which is also within an acceptable range. There are some high values of the aspect ratio in the draft tube due to quite long cells at the end of the draft tube.

Table 14 – Mesh statistics, $\underline{u}_1$=0.8

Domain name	Orthogonal Angle Minimum [deg]	Expansion Factor Maximum	Aspect Ratio Maximum
Draft tube	51.6 (100 %OK)	2 (100 %OK)	2033 (3 %!, 15 %ok, 82%OK)
Inflow	80.1 (100 %OK)	2 (100 %OK)	318 (14 %ok, 86 %OK)
Runner	45.9 (2 %ok, 98 % OK)	5 (100 %OK)	204 (<1 %ok, 100 %OK)
Global	45.9 (2 %ok, 98 % OK)	5 (100 %OK)	2033 (<1 %!, 2 %ok, 98 %OK)